

## Electronic Supplementary Information

# Bis-Urea Macrocycles with a Deep Cavity

Guobao Huang,<sup>a,b</sup> Zhenfeng He,<sup>b,d</sup> ChenXi Cai,<sup>b</sup> Fangfang Pan,<sup>c</sup> Dingqiao Yang,<sup>\*a</sup> Kari Rissanen,<sup>c</sup> and Wei Jiang<sup>\*b</sup>

*a School of Chemistry and Environment, South China Normal University(SCNU), Guangzhou, 510006, China*

*\*E-mail: [yangdq@scnu.edu.cn](mailto:yangdq@scnu.edu.cn)*

*b Department of Chemistry, South University of Science and Technology of China(SUSTC), Shenzhen, 518055, China*

*\*E-mail: [jiangw@sustc.edu.cn](mailto:jiangw@sustc.edu.cn)*

*c Department of Chemistry, Nanoscience Center, P.O. Box. 35, FI-40014 University of Jyväskylä, Finland*

*d School of Chemical Engineering and Environment, North University of China, No.3 Xueyuan Road, Taiyuan, Shanxi, 030051, P. R. China.*

### Table of Contents

1. General Methods	S2
2. Synthetic Procedures	S3
3. <sup>1</sup> H, <sup>1</sup> H-ROESY NMR Spectra of <b>1-anti</b> and <b>1-syn</b>	S9
4. Single Crystal Structures	S11
5. NMR Spectra of Host-Guest Complexes	S15
6. Job's Plots	S26
7. Determination of Binding Constants	S28

## 1. General Methods

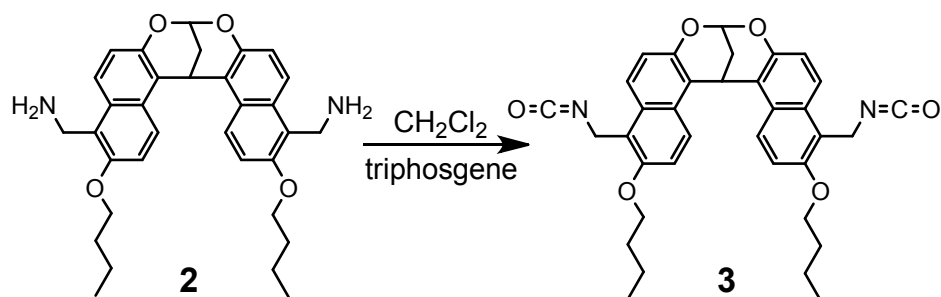
All the reagents and guest molecules involved in this research were commercially available and used without further purification unless otherwise noted. Solvents were either employed as purchased or dried prior to use by standard laboratory procedures. Thin-layer chromatography (TLC) was carried out on 0.25 mm Yantai silica gel plates (60F-254). Column chromatography was performed on silica gel 60 (Tsingdao 40 – 63 nm, 230 – 400 mesh).  $^1\text{H}$ ,  $^{13}\text{C}$ , and  $^1\text{H}, ^1\text{H}$ -ROESY NMR spectra were recorded on a Bruker Avance-400 NMR spectrometer. All chemical shifts are reported in *ppm* with residual solvents or TMS (tetramethylsilane) as the internal standards. The following abbreviations were used for signal multiplicities: s, singlet; d, doublet; dd, doublet of doublet; m, multiplet. Electrospray-ionization high-resolution mass spectrometry (ESI-HRMS) experiments were conducted on an applied Q EXACTIVE mass spectrometry system. All the computations were performed at the MMFF94 level of theory by using Spartan '14 (Wavefunction, Inc.). The synthesis of diamine **2**<sup>1</sup> has been reported.

---

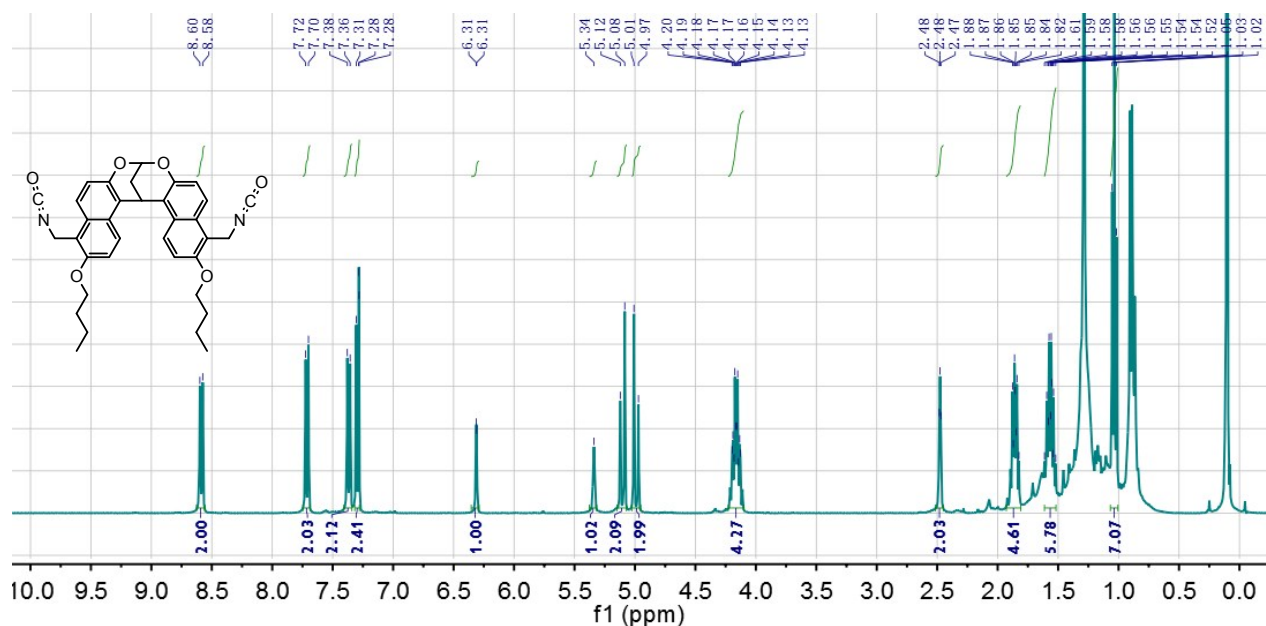
<sup>1</sup> Z. He, G. Ye and W. Jiang, *Chem. –Eur. J.* 2015, **21**, 3005-3012.

## 2. Synthetic Procedures

### Compound 3

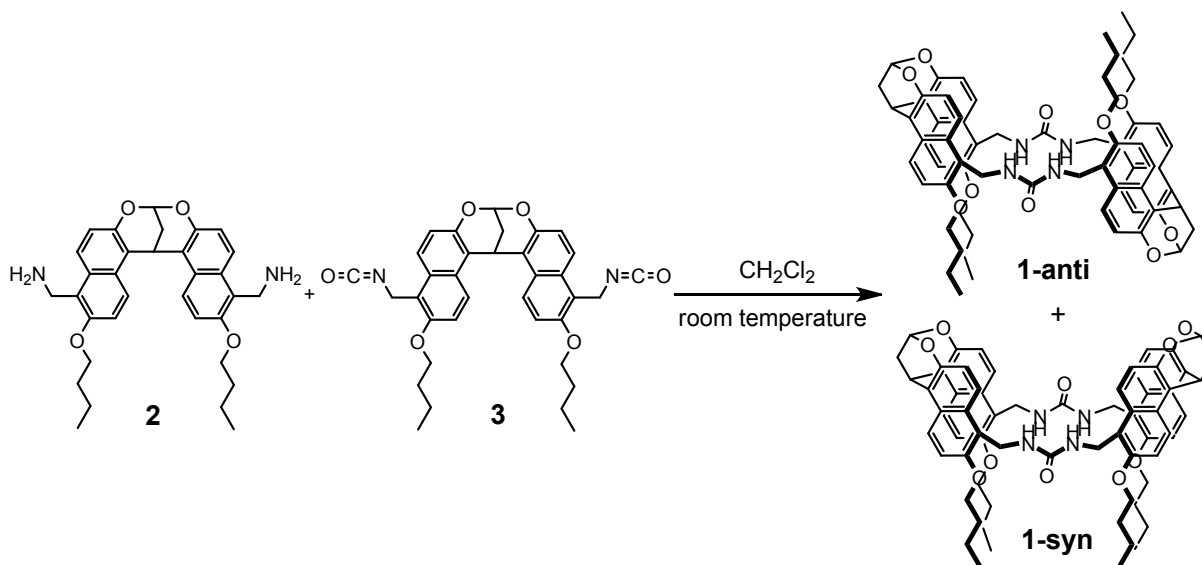


To the solution of triphosgene (178 mg, 0.6 mmol) in DCM (100 mL), were added compound **2** (210 mg, 0.4 mmol) and Hünig's base were added dropwise during 30 min. The resulting mixture was stirred at room temperature for 4 h. The solvent was removed in vacuum, and the residue was purified by column chromatography ( $\text{SiO}_2$ , hexane) to give the compound **3** as a yellow solid (208 mg, 90 %).  $^1\text{H}$  NMR (400 MHz,  $\text{CDCl}_3$ , 25 °C):  $\delta$  [ppm] = 8.56 (d,  $J = 9.4$  Hz, 2H), 7.69 (d,  $J = 9.2$  Hz, 2H), 7.34 (d,  $J = 9.4$  Hz, 2H), 7.26 (d,  $J = 9.2$  Hz, 2H), 6.29 (s, 1H), 5.32 (s, 1H), 5.02 (dd,  $J = 13.0, 4.1$  Hz, 2H), 4.23-4.07 (m, 4H), 2.45 (s, 2H), 1.74-1.82 (m, 4H), 1.62-1.42 (m, 4H), 1.01 (t,  $J = 7.4$  Hz, 6H).



$^1\text{H}$  NMR spectrum (400 MHz,  $\text{CDCl}_3$ , 25 °C) of compound **3**.

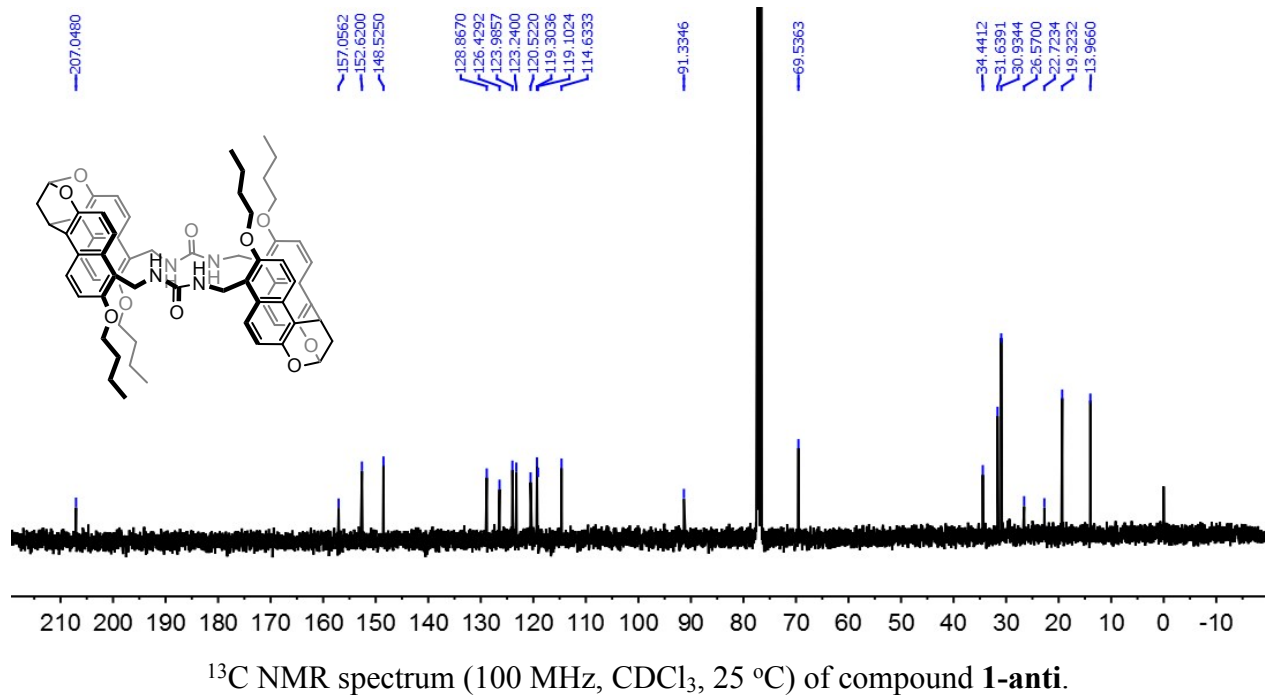
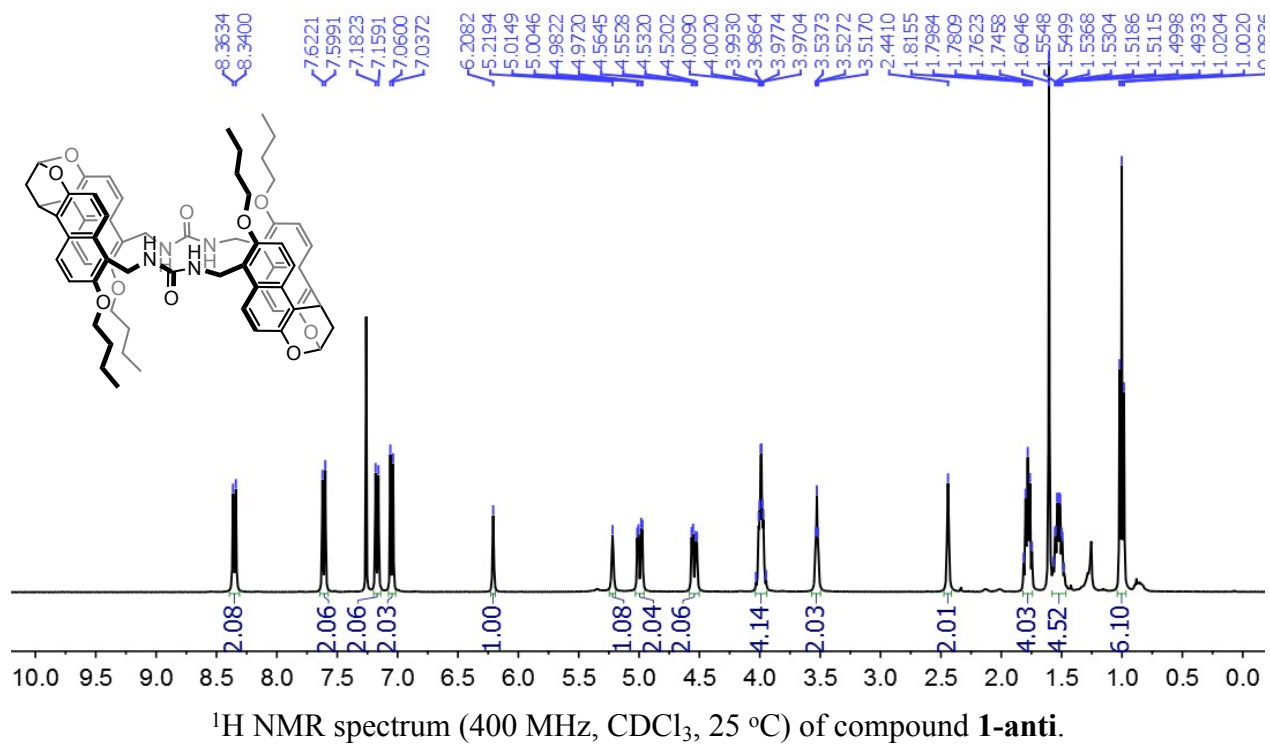
## Compound 1-anti/1-syn



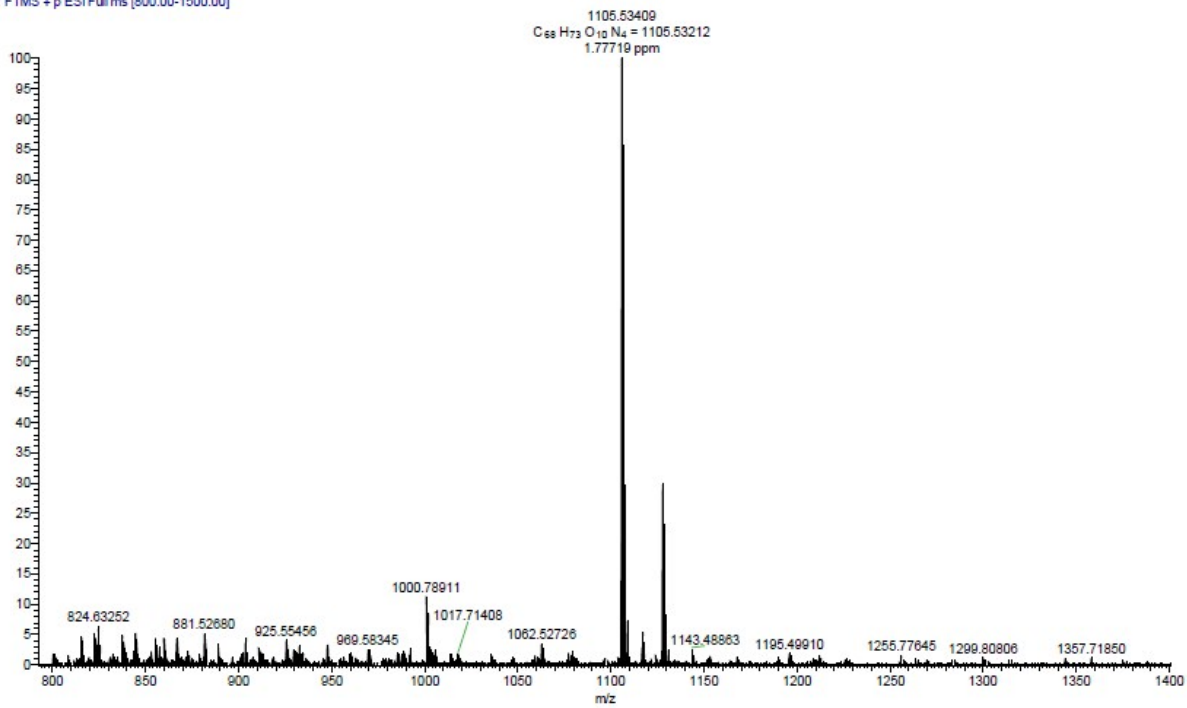
## Compound 1-anti/1-syn

The solutions of compounds **2** (210 mg, 0.4 mmol; in 60 mL DCM) and **3** (231 mg, 0.4 mmol; in 60 mL DCM) in two separate syringes were added dropwise via a double-channel syringe pump to the solution of Hünig's base (258 mg, 2.0 mmol) in DCM (200 mL) during the course of 10 h. The resulting mixture was stirred overnight at room temperature. After removing the solvent in vacuum, the residue was subjected to column chromatography (SiO<sub>2</sub>, CH<sub>3</sub>OH / DCM = 1 / 100) to afford the two isomers of macrocycle **1**.

**1-anti**. White solid; yield, 110 mg, 25%; m.p. > 360 °C (Decomposed); <sup>1</sup>H NMR (400 MHz, CDCl<sub>3</sub>, 25 °C): δ [ppm] = 8.35 (d, *J* = 9.4 Hz, 2H), 7.61 (d, *J* = 9.2 Hz, 2H), 7.17 (d, *J* = 9.4 Hz, 2H), 7.05 (d, *J* = 9.2 Hz, 2H), 6.21 (s, 1H), 5.22 (s, 1H), 5.00 (dd, *J* = 13.0, 4.1 Hz, 2H), 4.55 (dd, *J* = 13.0, 4.1 Hz, 2H), 4.00 (t, *J* = 3.8 Hz, 4H), 3.53 (t, *J* = 9.4 Hz, 2H), 2.44 (s, 2H), 1.74-1.82 (m, 4H), 1.62-1.42 (m, 4H), 1.01 (t, *J* = 7.4 Hz, 6H). <sup>13</sup>C NMR (100 MHz, CDCl<sub>3</sub>, 25 °C): δ [ppm] = 207.1, 157.1, 152.6, 148.5, 128.8, 126.4, 124.0, 123.2, 120.5, 119.3, 119.1, 114.6, 91.3, 69.5, 34.4, 31.6, 30.9, 26.6, 22.7, 19.3, 14.0. ESI-TOF-HRMS: *m/z* calcd for [M+H]<sup>+</sup> C<sub>68</sub>H<sub>73</sub>N<sub>4</sub>O<sub>10</sub><sup>+</sup>, 1105.5321; found 1105.5341 (100%).

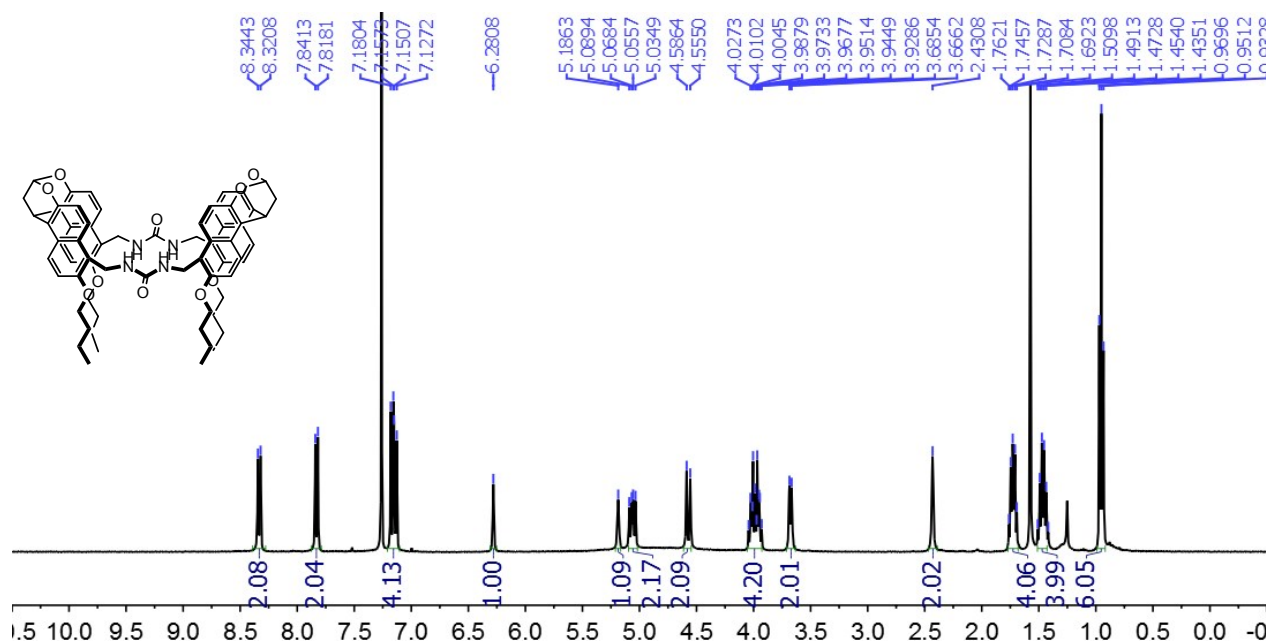


1-anti #16 RT: 0.07 AV: 1 SB: 125 0.32-0.87 NL: 4.02E6  
T: FTMS + p ESI Full ms [800.00-1500.00]

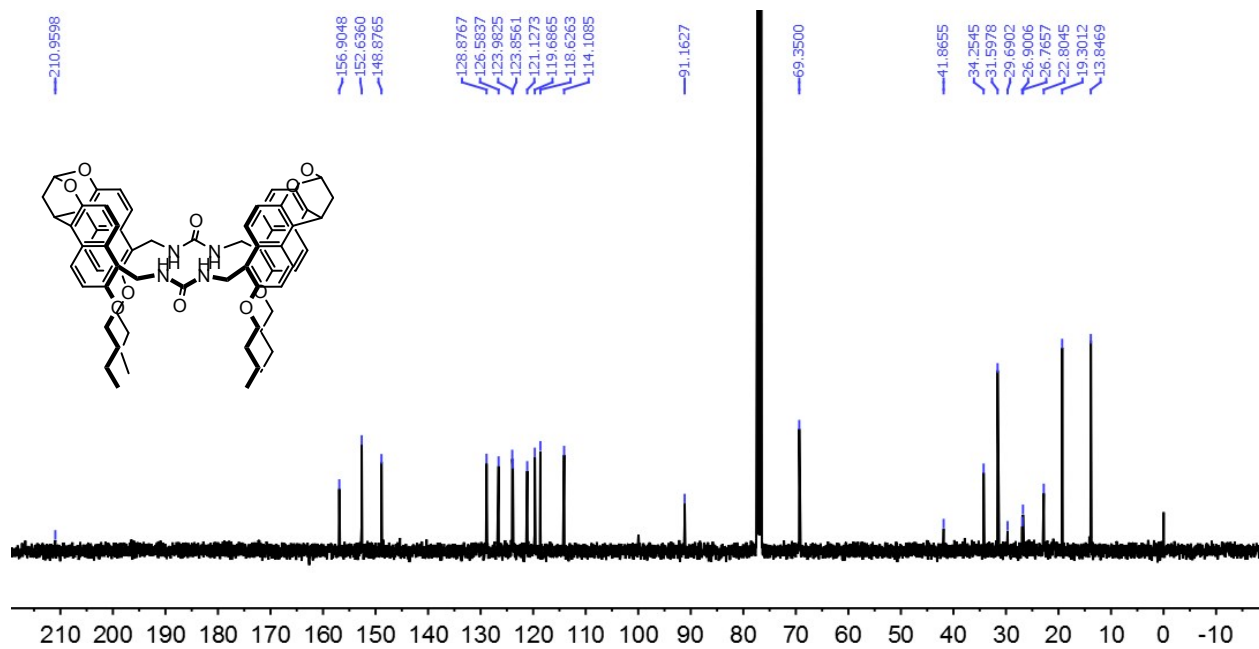


ESI mass spectrum of compound **1-anti**.

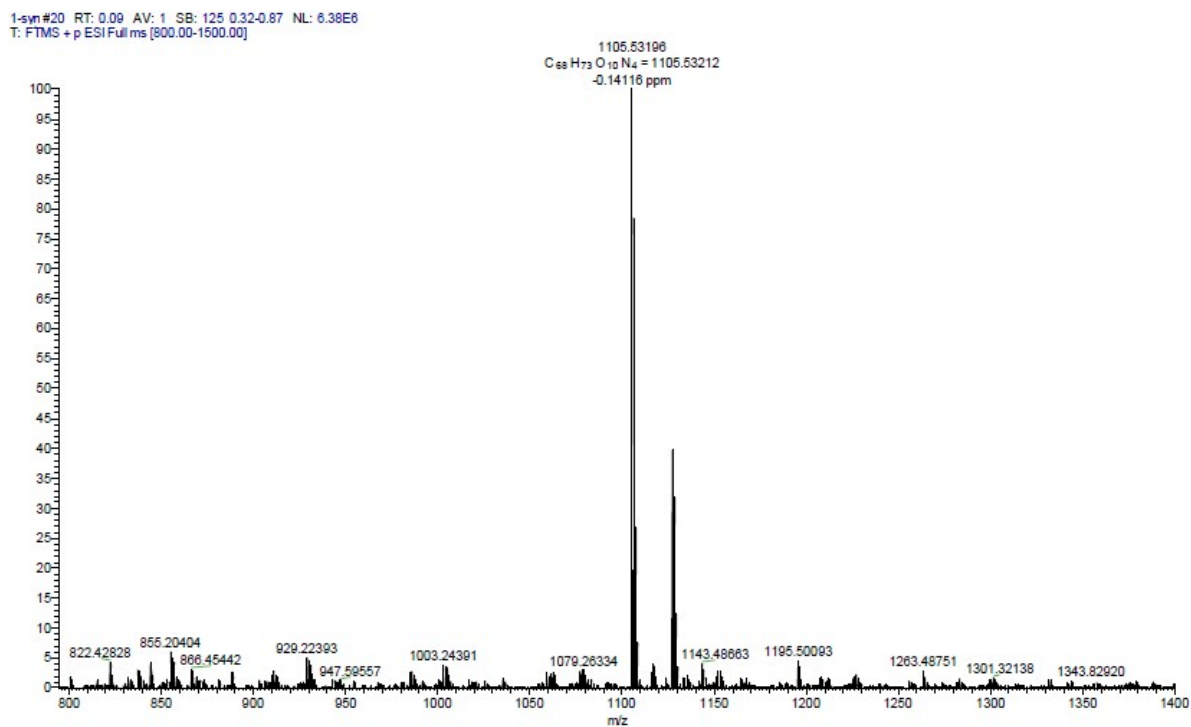
**1-syn.** White solid; yield, 114 mg, 26%; m.p. > 360 °C (Decomposed); <sup>1</sup>H NMR (400 MHz, CDCl<sub>3</sub>, 25 °C): δ [ppm] = 8.33 (d, *J* = 9.4 Hz, 2H), 7.83 (d, *J* = 9.3 Hz, 2H), 7.15 (dd, *J* = 11.4, 9.5 Hz, 4H), 6.28 (s, 1H), 5.18 (s, 1H), 5.06 (dd, *J* = 13.2, 8.4 Hz, 2H), 4.57 (d, *J* = 13.2 Hz, 2H), 3.92-4.04 (m, 4H), 3.68 (d, *J* = 7.7 Hz, 2H), 2.43 (s, 2H), 1.68-1.75 (m, 4H), 1.41-1.50 (m, 4H), 0.95 (t, *J* = 7.4 Hz, 6H). <sup>13</sup>C NMR (100 MHz, CDCl<sub>3</sub>, 25 °C): δ [ppm] = 206.2, 156.9, 152.6, 148.9, 128.9, 126.6, 124.0, 123.9, 121.2, 119.7, 118.6, 114.1, 91.2, 69.4, 34.3, 31.6, 29.7, 26.8, 22.8, 19.3, 13.8. ESI-TOF-HRMS: *m/z* calcd for [M+H]<sup>+</sup> C<sub>68</sub>H<sub>73</sub>N<sub>4</sub>O<sub>10</sub><sup>+</sup>, 1105.5321; found 1105.5320 (100%).



<sup>1</sup>H NMR spectrum (400 MHz, CDCl<sub>3</sub>, 25 °C) of compound **1-syn**.



$^{13}\text{C}$  NMR spectrum (100 MHz,  $\text{CDCl}_3$ , 25 °C) of compound **1-syn**.



ESI mass spectrum of compound **1-syn**.

### 3. $^1\text{H}$ , $^1\text{H}$ -ROESY NMR Spectra of **1-anti** and **1-syn**.

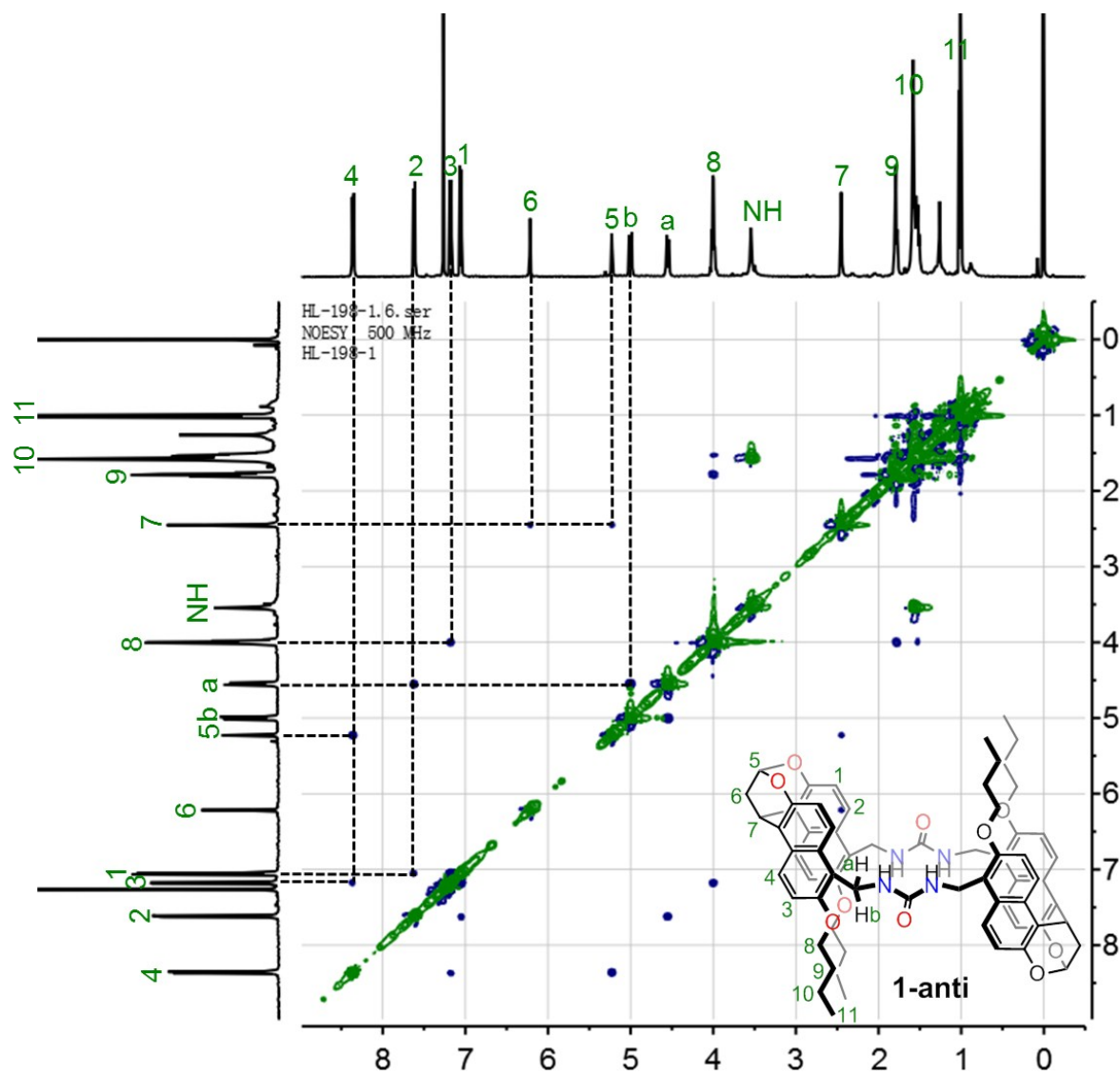


**Fig. S1**  $^1\text{H}$ ,  $^1\text{H}$ -ROESY NMR spectrum (400 MHz,  $\text{CDCl}_3$ , 25  $^\circ\text{C}$ ) of compound **1-anti**.

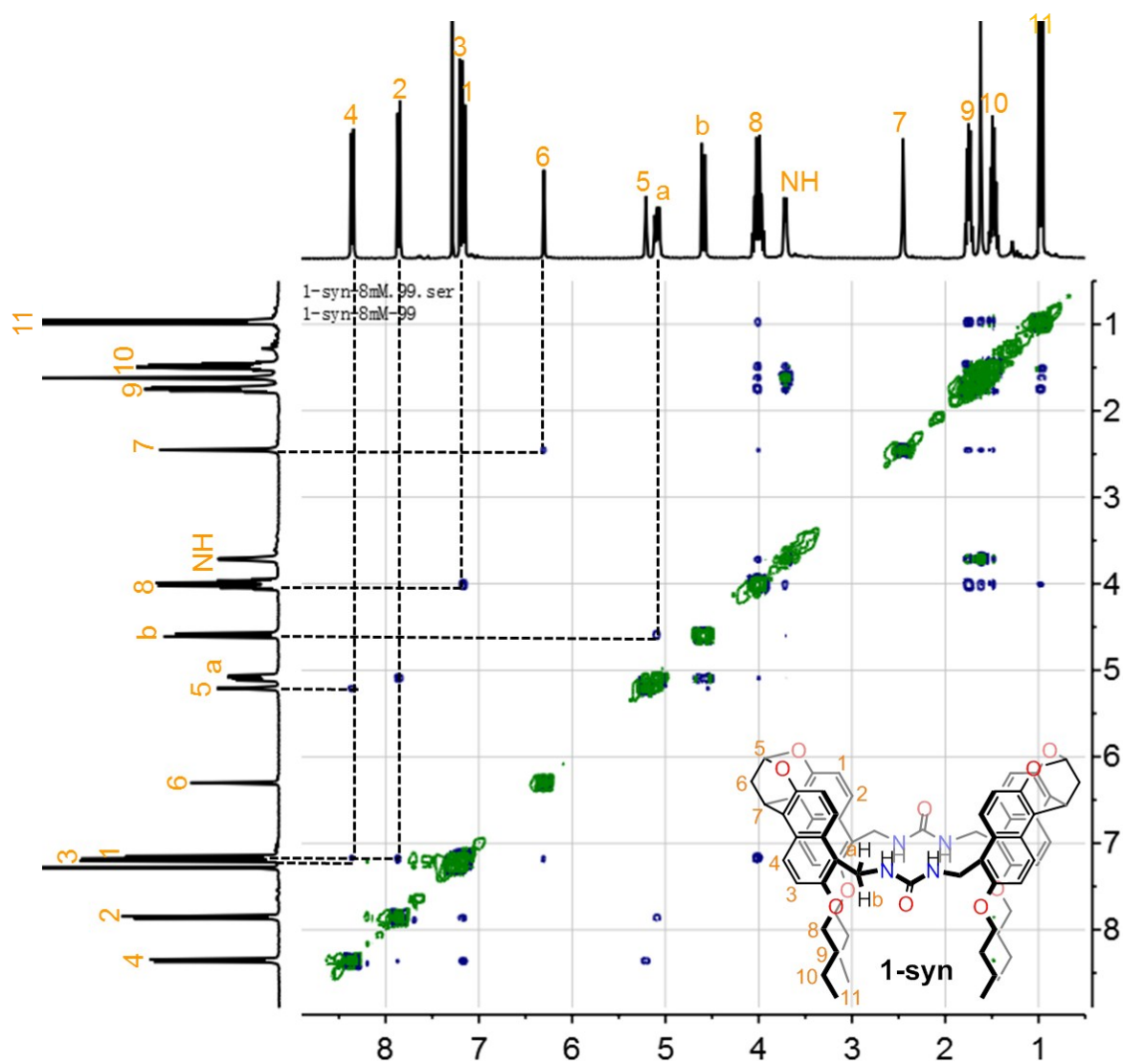


**Fig. S2**  $^1\text{H}$ ,  $^1\text{H}$ -ROESY NMR spectrum (400 MHz,  $\text{CDCl}_3$ , 25  $^\circ\text{C}$ ) of compound **1-syn**.

## 4. Single Crystal Structures

Single crystal X-ray data for **4@1-syn** was collected at 100.01(10) K using an Agilent Super-Nova diffractometer with a mirror-monochromatized Mo- $K\alpha$  ( $\lambda = 0.71073 \text{ \AA}$ ) radiation, while data collection for **CH<sub>3</sub>CN@1-anti**, **CH<sub>3</sub>CN@1-syn**, and **4@1-anti** was performed at 123.01(10) K with Agilent Super-Nova dual wavelength diffractometer with a micro-focus X-ray source and multilayer optics monochromatized Cu- $K\alpha$  ( $\lambda = 1.54184 \text{ \AA}$ ) radiation. Program *CrysAlisPro*<sup>3</sup> was used for the data collection and reduction. The intensities were corrected for absorption using analytical face index absorption correction method<sup>4</sup> for all the data. The structures were solved with direct methods (*SHELXS*<sup>5</sup>) and refined by full-matrix least squares on  $F^2$  using the *OLEX2*<sup>6</sup>, which utilizes the *SHELXL-2013* module<sup>5</sup>. Anisotropic displacement parameters were assigned to non-H atoms. All the hydrogen atoms were refined using riding models with  $U_{eq}(\text{H})$  of  $1.5U_{eq}(\text{parent})$  for hydroxyl and terminal methyl groups, and  $1.2U_{eq}(\text{parent})$  for other groups., Two of the butyl groups in **CH<sub>3</sub>CN@1-anti**, **CH<sub>3</sub>CN@1-syn** and **4@1-syn**, and all the four butyl groups in **4@1-anti** are disordered. They were split over two positions according to the difference Fourier maps. In addition, some solvent molecules also suffer disorder problem in these structures, they were treated accordingly based on the difference Fourier maps as well. Anisotropic displacement parameters and geometry of the disordered groups were constrained or restrained if necessary. The details of the crystals data, data collection, and the refinement results are documented in Table S1.

**Table S1.** Crystal data and structure refinement for **CH<sub>3</sub>CN@1-anti**, **CH<sub>3</sub>CN@1-syn**, **4@1-anti** and **4@1-syn**.

Crystal data	CH <sub>3</sub> CN@1-anti	CH <sub>3</sub> CN@1-syn	4@1-anti	4@1-syn
CCDC depos. No.	1417788	1417789	1417790	1417791
Chemical formula	C <sub>68</sub> H <sub>70</sub> N <sub>4</sub> O <sub>10</sub> ·7.7(C <sub>2</sub> H <sub>3</sub> N)·0.3(CH <sub>2</sub> Cl <sub>2</sub> )·2(H <sub>2</sub> O)	C <sub>68</sub> H <sub>72</sub> N <sub>4</sub> O <sub>10</sub> ·2.5(C <sub>2</sub> H <sub>3</sub> N)·CH <sub>2</sub> Cl <sub>2</sub> ·2(H <sub>2</sub> O)	C <sub>68</sub> H <sub>72</sub> N <sub>4</sub> O <sub>10</sub> ·C <sub>4</sub> H <sub>8</sub> O <sub>2</sub> ·2(CHCl <sub>3</sub> )	C <sub>68</sub> H <sub>72</sub> N <sub>4</sub> O <sub>10</sub> ·2.6(C <sub>4</sub> H <sub>8</sub> O <sub>2</sub> )·1.4(CH <sub>2</sub> Cl <sub>2</sub> )
<i>M<sub>r</sub></i>	1480.90	1431.52	1432.13	1453.26
Crystal system, space group	Triclinic, <i>P</i> -1	Orthorhombic, <i>Pnma</i>	Triclinic, <i>P</i> -1	Monoclinic, <i>P2</i> / <i>n</i>
Temperature (K)	123.0(1)	123.0(1)	123.0(1)	100.0(1)
<i>a</i>	11.6914(4)	23.8532(2)	11.992(4)	12.4884(7)
<i>b</i>	13.3995(3)	16.5865(2)	12.642(5)	17.1551(9)
<i>c</i> (Å)	13.6649(5)	19.1371(2)	13.390(4)	17.3844(8)
α, β, γ (°)	105.227(3), 99.554(3), 102.607(2)	90, 90, 90	78.03(3), 69.89(3), 65.52(3)	90, 96.545(4), 90
<i>V</i> (Å <sup>3</sup> )	1958.3(1)	7571.5(1)	1730(1)	3700.2(3)
<i>Z</i>	1	4	1	2
Radiation type	Cu <i>K</i> α	Cu <i>K</i> α	Mo <i>K</i> α	Mo <i>K</i> α
μ (mm <sup>-1</sup> )	0.87	1.31	0.31	0.19
Crystal size (mm)	0.36 × 0.31 × 0.10	0.29 × 0.25 × 0.10	0.11 × 0.07 × 0.06	0.55 × 0.16 × 0.03
<b>Data collection</b>				
<i>T</i> <sub>min</sub> , <i>T</i> <sub>max</sub>	0.698, 0.879	0.962, 0.983	0.993, 0.995	0.974, 0.997
No. of measured, independent and observed [ <i>I</i> > 2σ( <i>I</i> )] reflections	14442, 8014, 6943	26183, 8120, 6922	9961, 6199, 1655	42494, 6696, 4270
<i>R</i> <sub>int</sub>	0.031	0.034	0.116	0.089
(sin θ/λ) <sub>max</sub> (Å <sup>-1</sup> )	0.632	0.632	0.600	0.600
<b>Refinement</b>				
<i>R</i> [ <i>F</i> <sup>2</sup> > 2σ( <i>F</i> <sup>2</sup> )], <i>wR</i> ( <i>F</i> <sup>2</sup> ), <i>S</i>	0.068, 0.208, 1.04	0.069, 0.208, 1.03	0.111, 0.345, 0.96	0.077, 0.227, 1.05
No. of reflections	8014	8120	6199	6696
No. of parameters	530	627	499	517
No. of restraints	0	62	330	45
H-atom treatment	mixture of independent and constrained refinement	mixture of independent and constrained refinement	constrained	constrained
Δρ <sub>max</sub> , Δρ <sub>min</sub> (e Å <sup>-3</sup> )	0.60, -0.46	1.16, -0.90	0.47, -0.56	0.31, -0.41

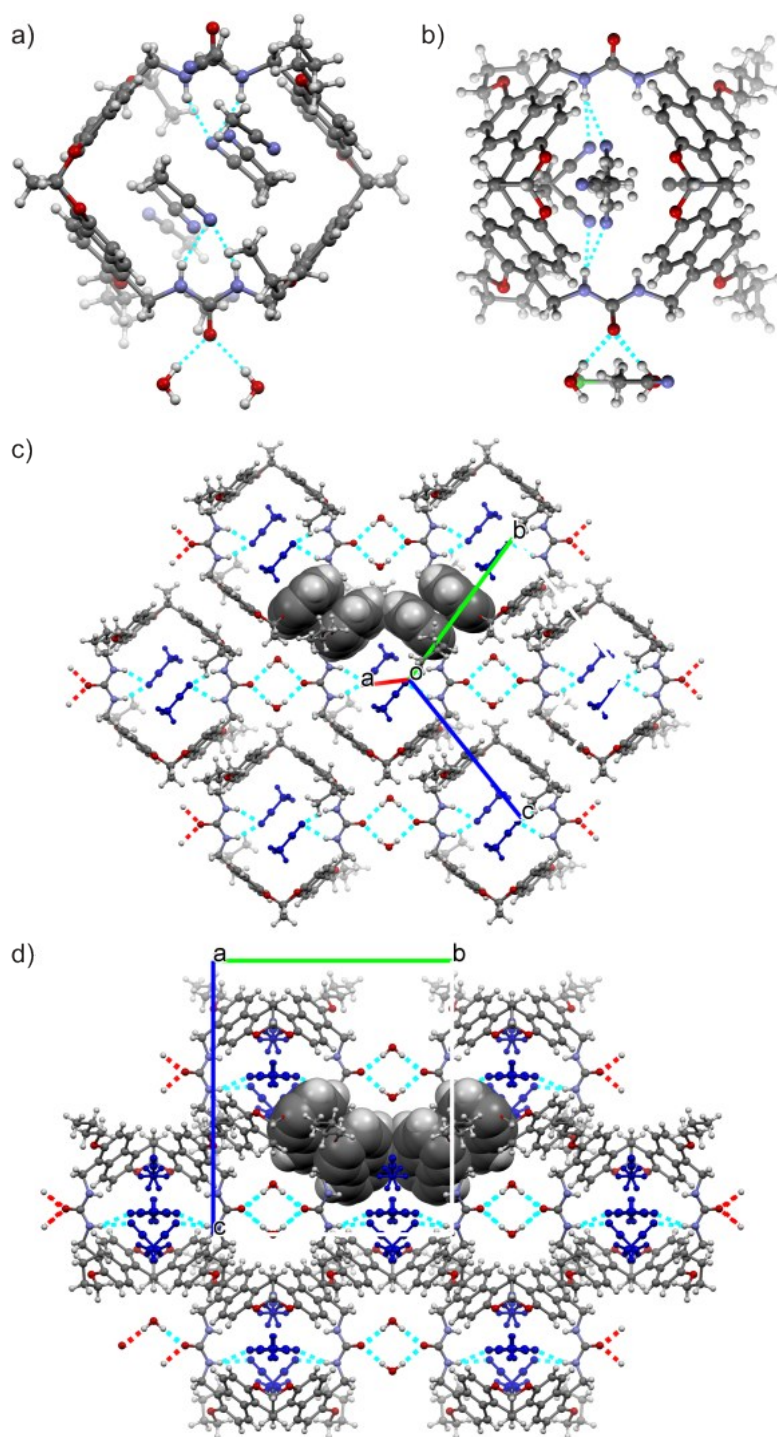


**Fig. S3** The structural composition of (a) **1-anti** and (b) **1-syn** obtained from the solution in the mixture of CH<sub>2</sub>Cl<sub>2</sub> and CH<sub>3</sub>CN; Crystal packing of (c) **1-anti** and (d) **1-syn** via hydrogen bonds and π···π stacking (highlighted in CPK model). The in-cavity solvent molecules are drawn in blue and the out-of-cavity solvents omitted for clarity.

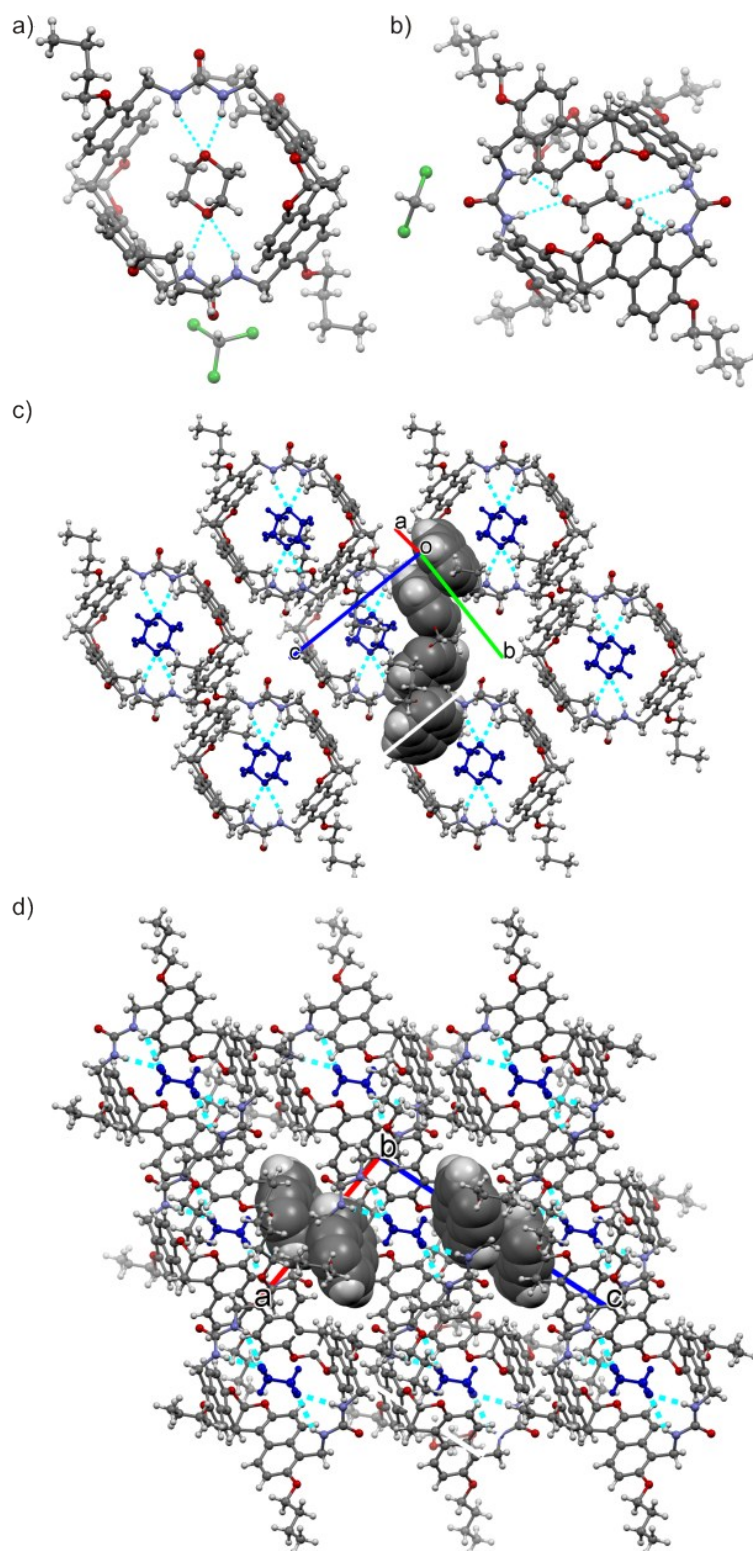


**Fig. S4** The structural composition in (a) **4@1-anti** and (b) **4@1-syn**. In the crystal packing of (c) **4@1-anti** and (d) **4@1-syn**, the 1,4-dioxane molecules are drawn in blue with CPK model highlighting the  $\pi \cdots \pi$  interactions.

## 5. NMR Spectra of Host-Guest Complexes.

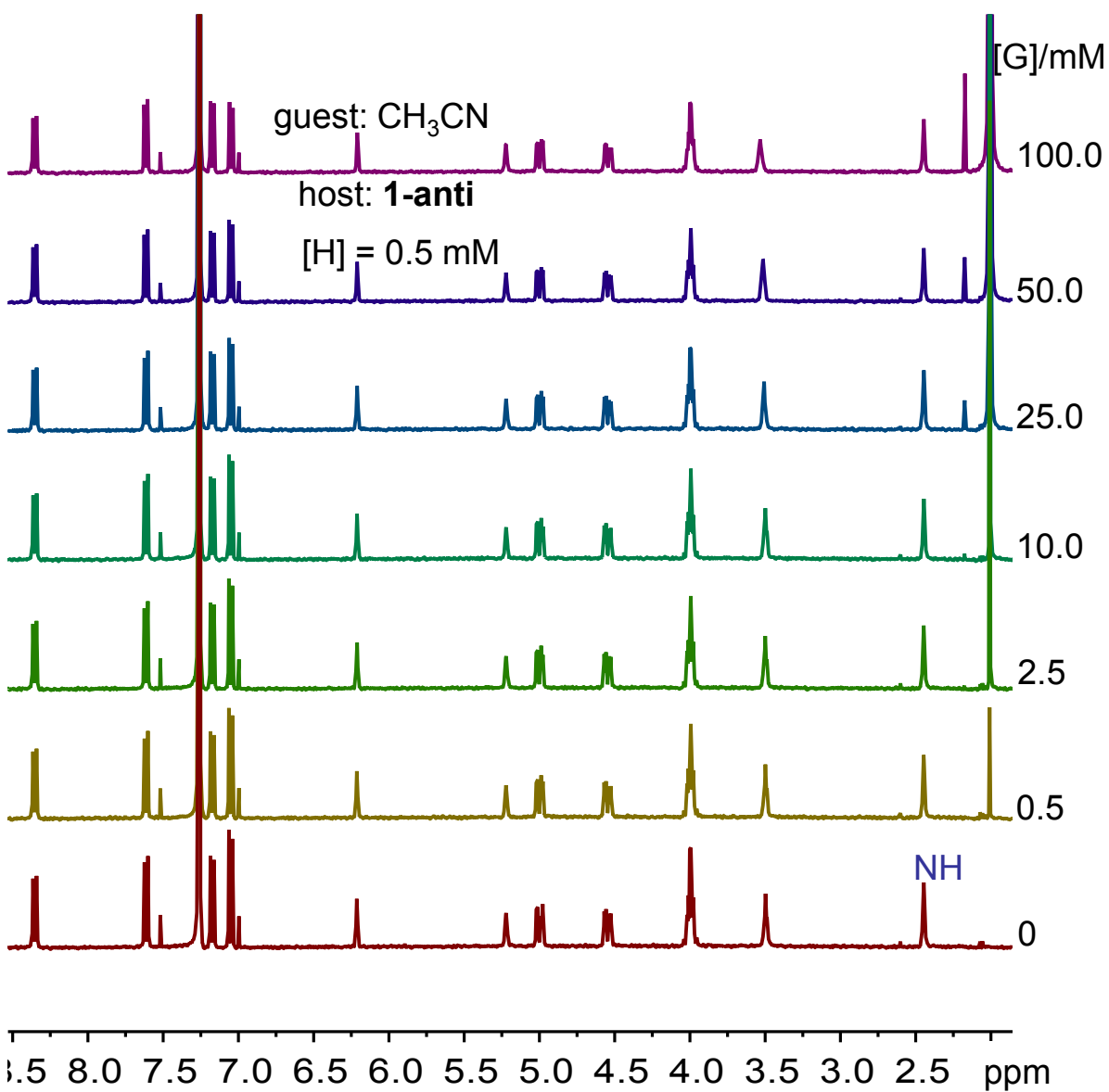


**Fig. S5** <sup>1</sup>H NMR spectra (400 MHz, CDCl<sub>3</sub>, 25 °C) of **1-anti** (0.5 mM) titrated by CH<sub>3</sub>CN (0~100.0 mM). No obvious change on NH protons was observed, suggesting very weak binding between **1-anti** and CH<sub>3</sub>CN in solution.

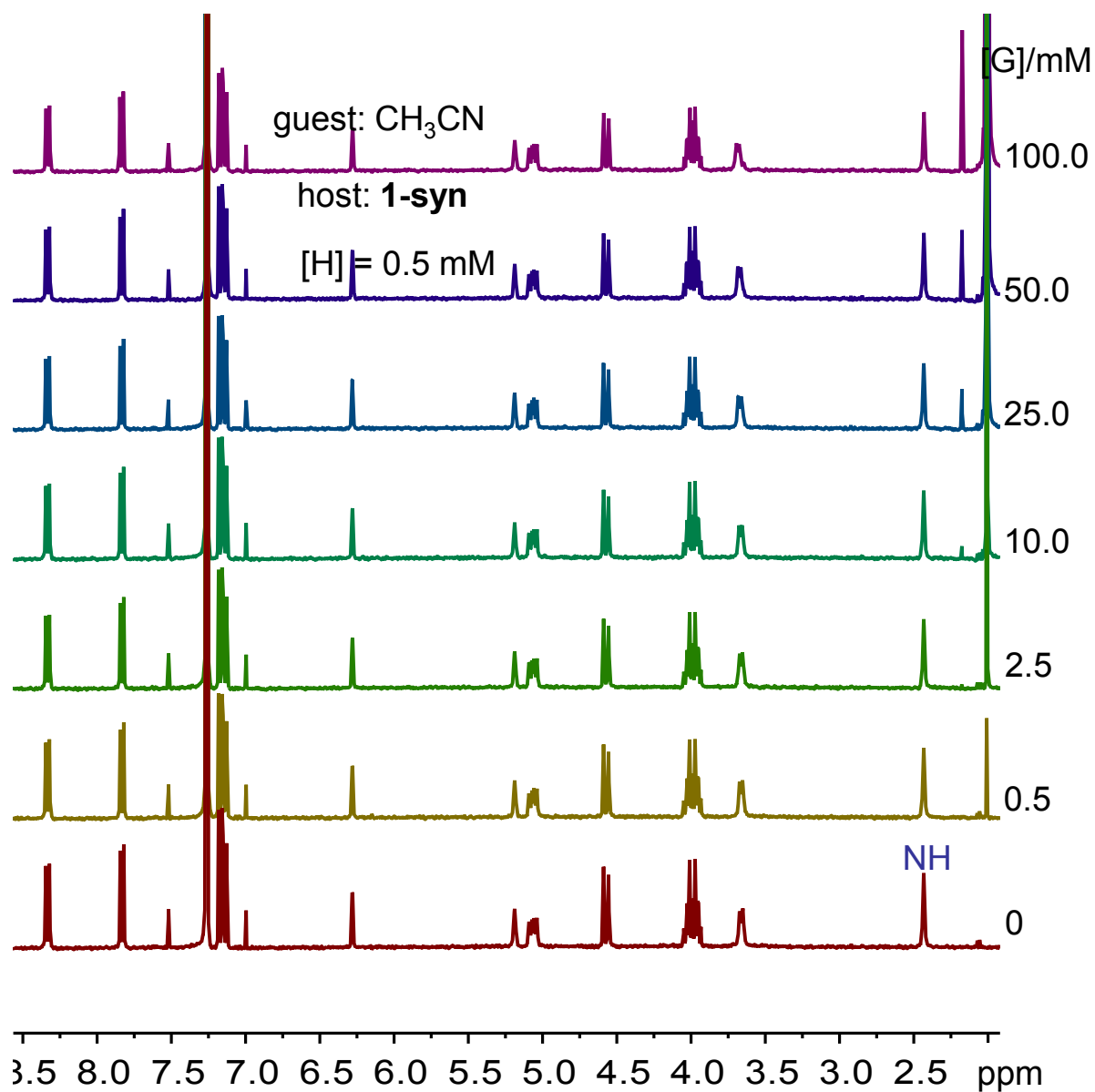


**Fig. S6** <sup>1</sup>H NMR spectra (400 MHz, CDCl<sub>3</sub>, 25 °C) of **1-syn** (0.5 mM) titrated by CH<sub>3</sub>CN (0~100.0 mM). No obvious change on NH protons was observed, suggesting very weak binding between **1-syn** and CH<sub>3</sub>CN in solution.

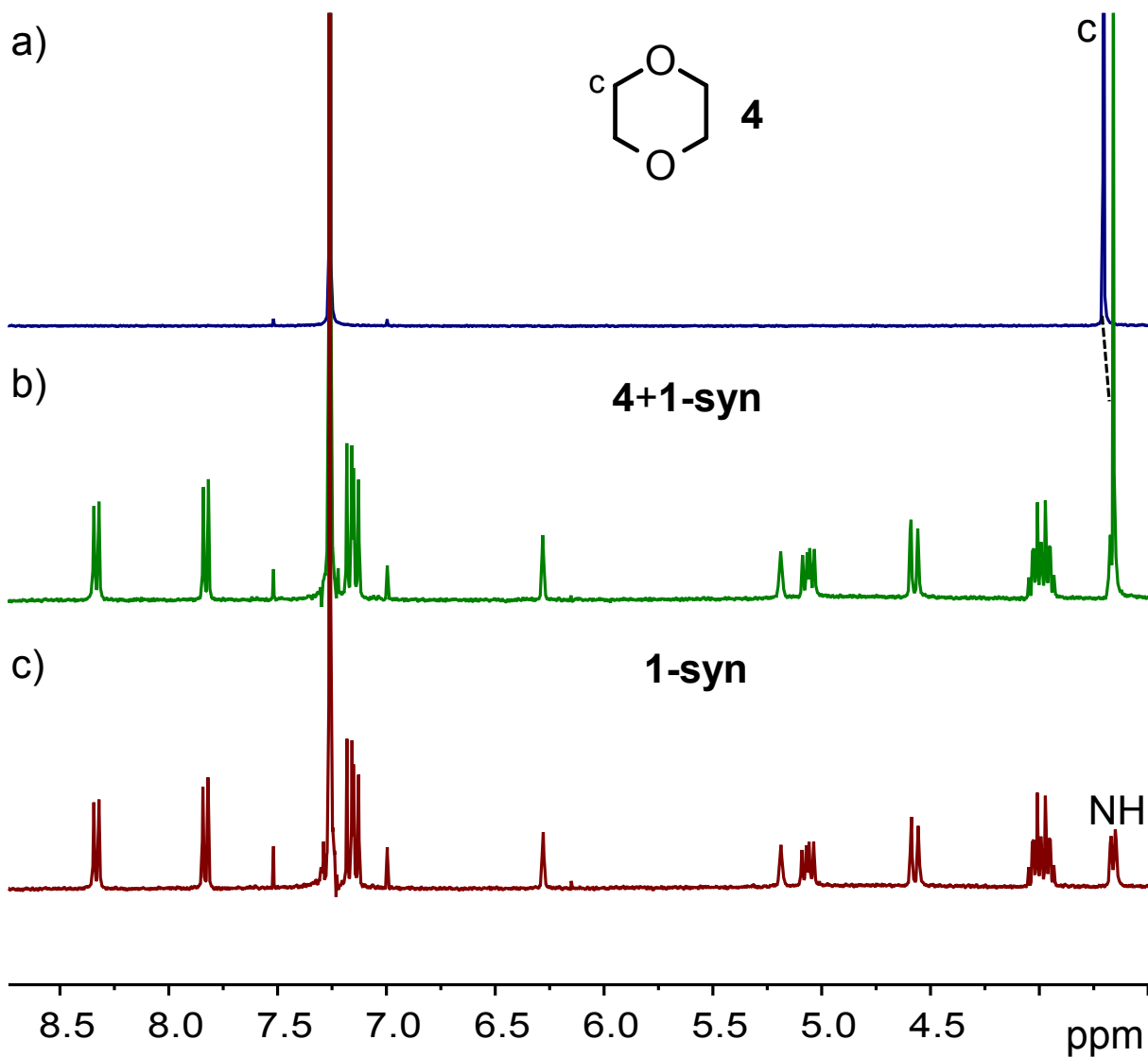


**Fig. S7** <sup>1</sup>H NMR spectra (400 MHz, CDCl<sub>3</sub>, 25 °C) of (a) guest **4**, (c) **1-syn**, and (b) its equimolar mixture. The proton *c* of the guest experiences the upfield shift, suggesting that the complexation between **1-syn** and guest **4**.

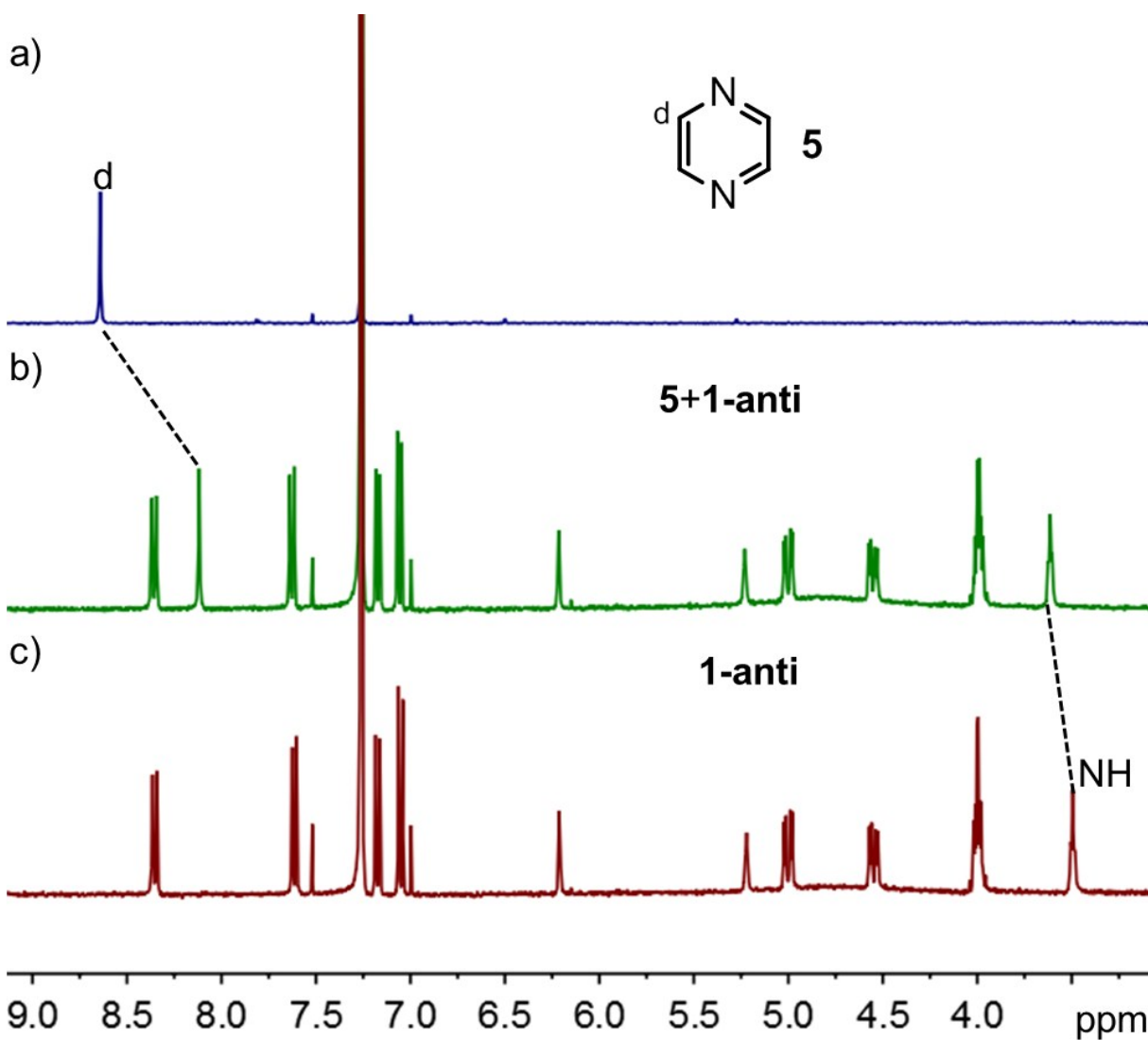


**Fig. S8** <sup>1</sup>H NMR spectra (400 MHz, CDCl<sub>3</sub>, 25 °C) of (a) guest **5**, (c) **1-anti**, and (b) its equimolar mixture. The proton *d* of the guest experiences the large upfield shift, the proton NH of the host experiences the downfield shift, suggesting that the complexation between **1-anti** and guest **5**.

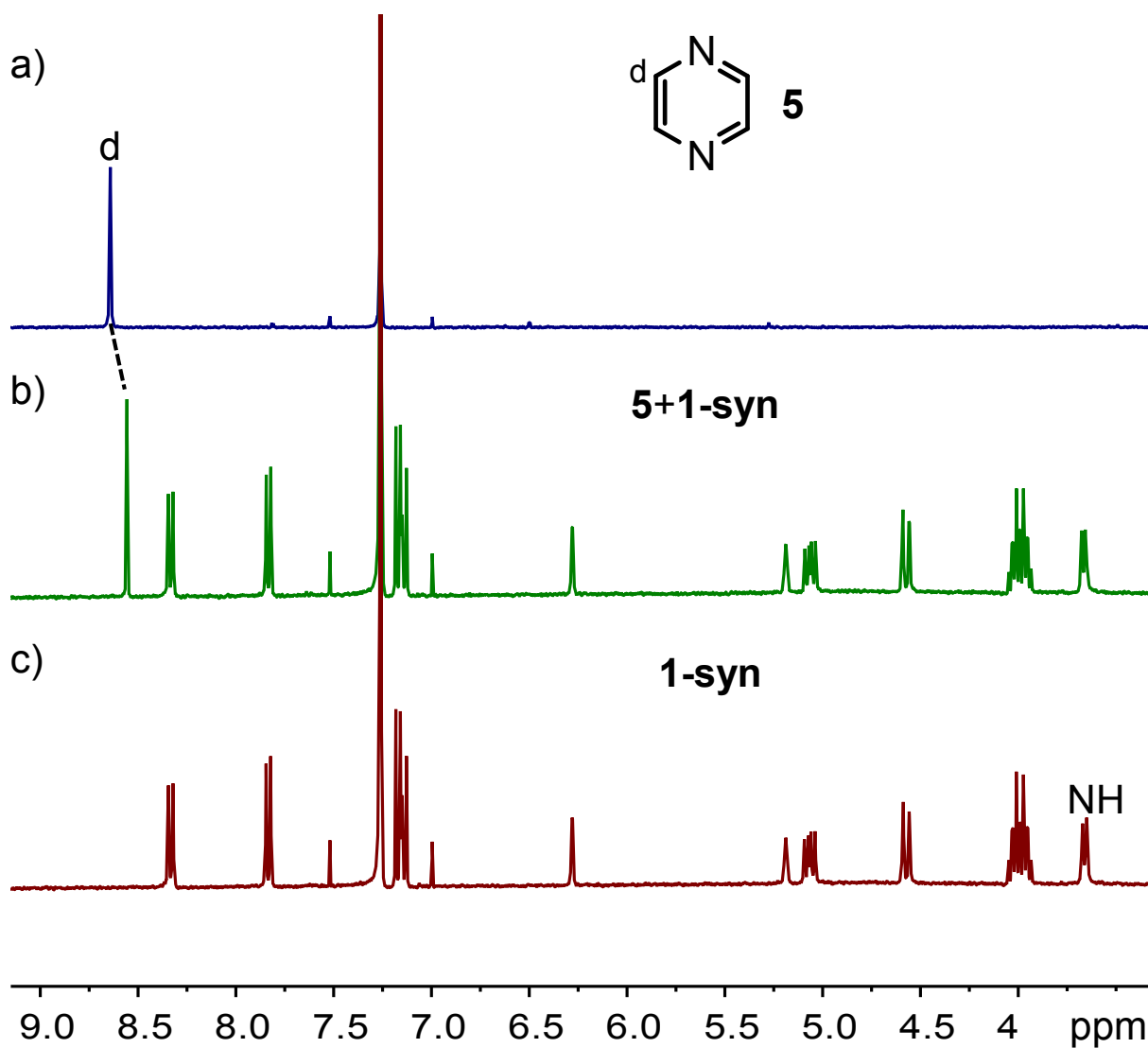


**Fig. S9** <sup>1</sup>H NMR spectra (400 MHz, CDCl<sub>3</sub>, 25 °C) of (a) guest **5**, (c) **1-syn**, and (b) its equimolar mixture. The proton *d* of the guest experiences the large upfield shift, suggesting that the complexation between **1-syn** and guest **5**.

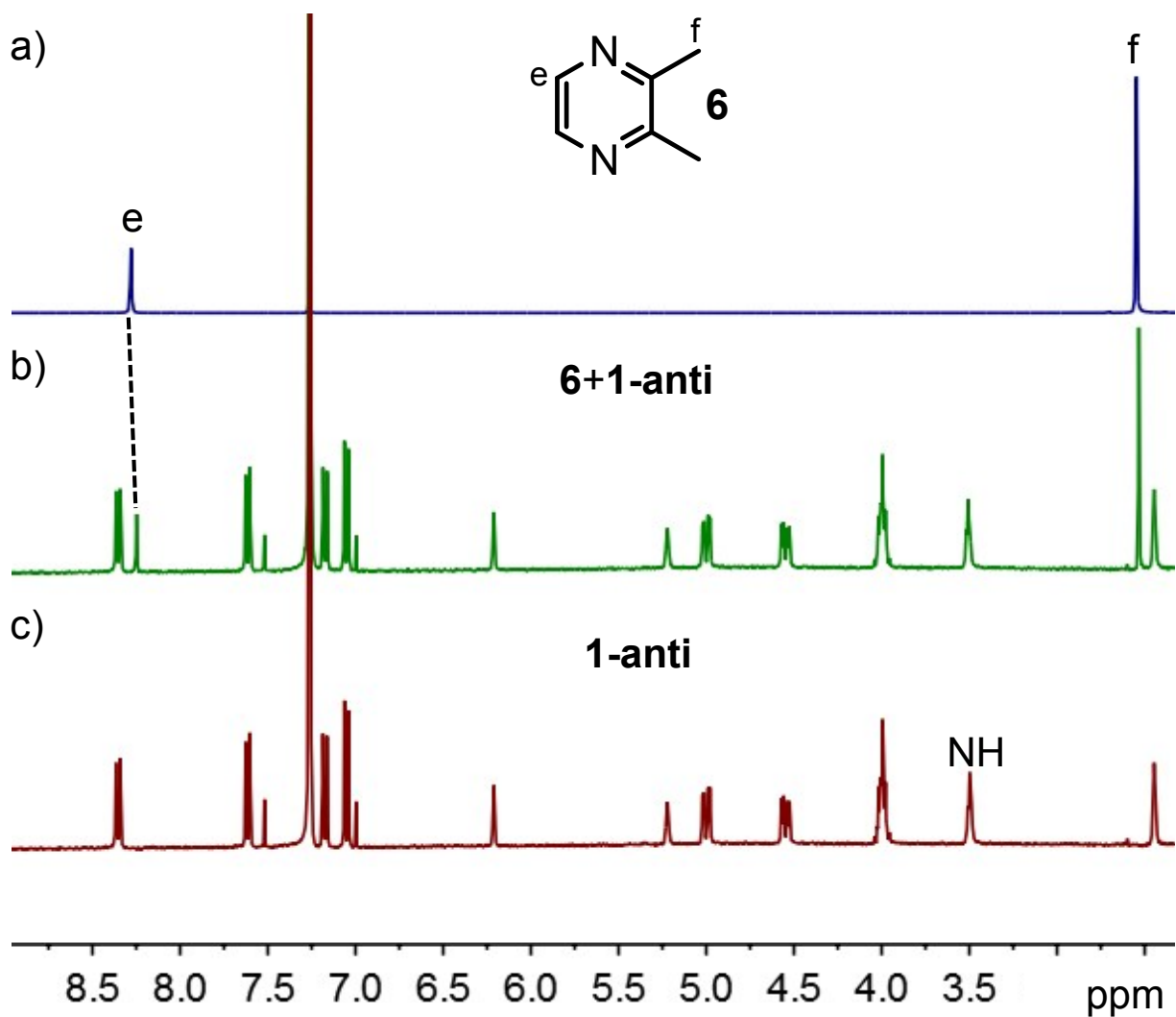


**Fig. S10** <sup>1</sup>H NMR spectra (400 MHz, CDCl<sub>3</sub>, 25 °C) of (a) guest **6**, (c) **1-anti**, and (b) its equimolar mixture. The proton *e* of the guest experiences the large upfield shift, suggesting that the complexation between **1-anti** and guest **6**.

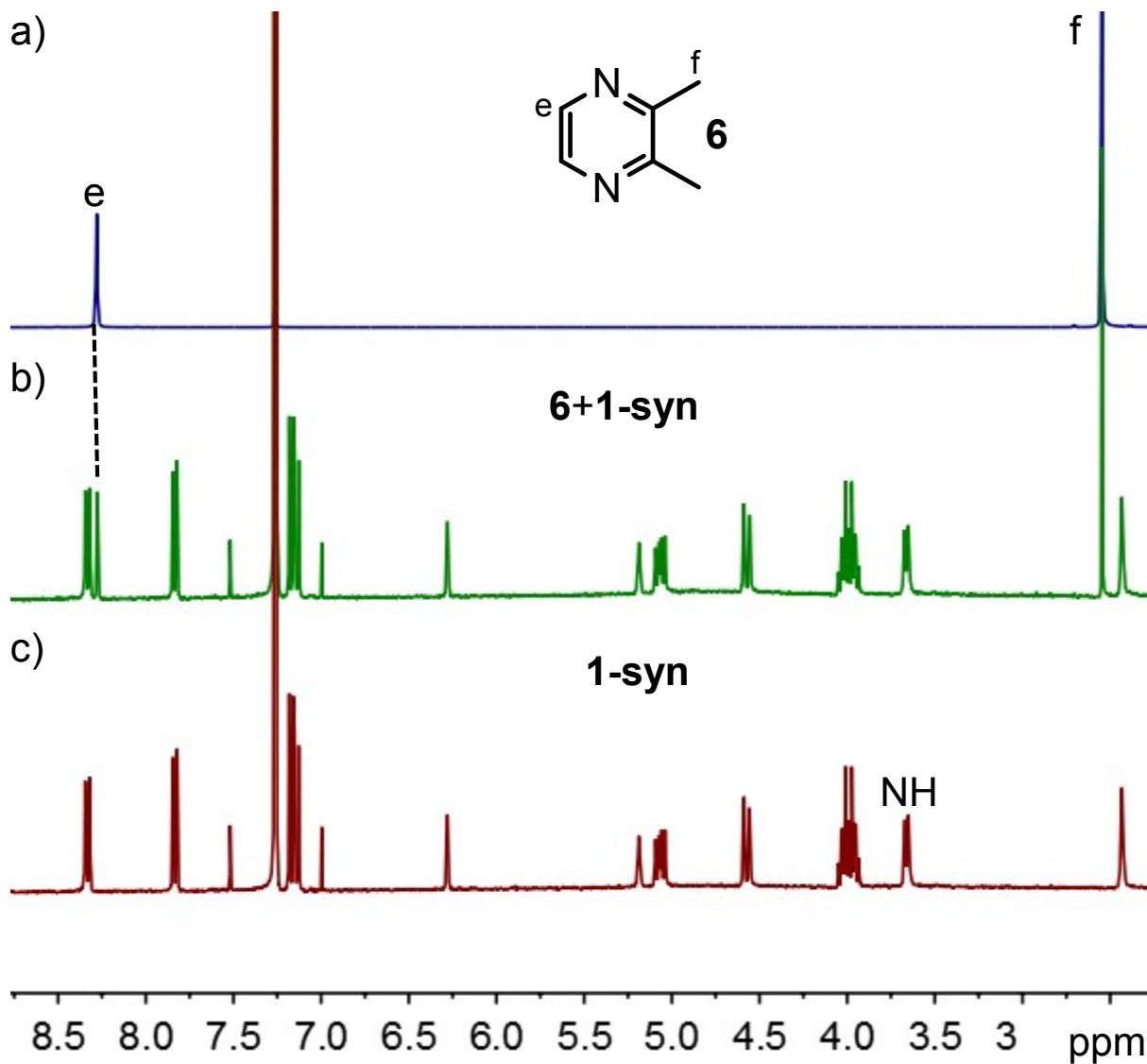


**Fig. S11** <sup>1</sup>H NMR spectra (400 MHz, CDCl<sub>3</sub>, 25 °C) of (a) guest **6**, (c) **1-syn**, and (b) its equimolar mixture. The proton *e* of the guest experiences the upfield shift, suggesting that the complexation between **1-syn** and guest **6**.

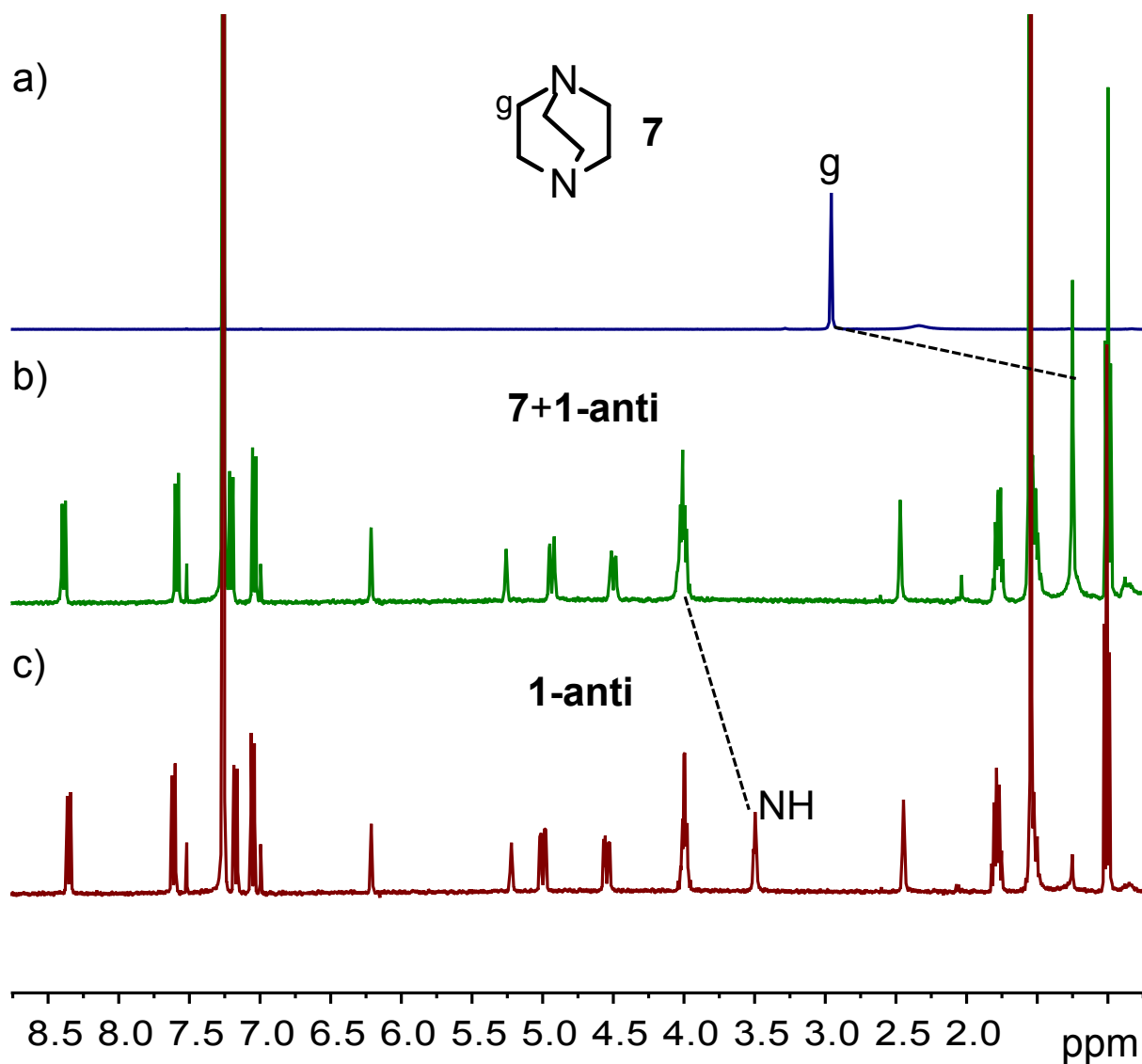


**Fig. S12**  $^1\text{H}$  NMR spectra (400 MHz,  $\text{CDCl}_3$ , 25  $^\circ\text{C}$ ) of (a) guest **7**, (c) **1-anti**, and (b) its equimolar mixture. The proton *g* of the guest experiences the large upfield shift, the proton NH of the host experiences the downfield shift, suggesting that the complexation between **1-anti** and guest **7**.

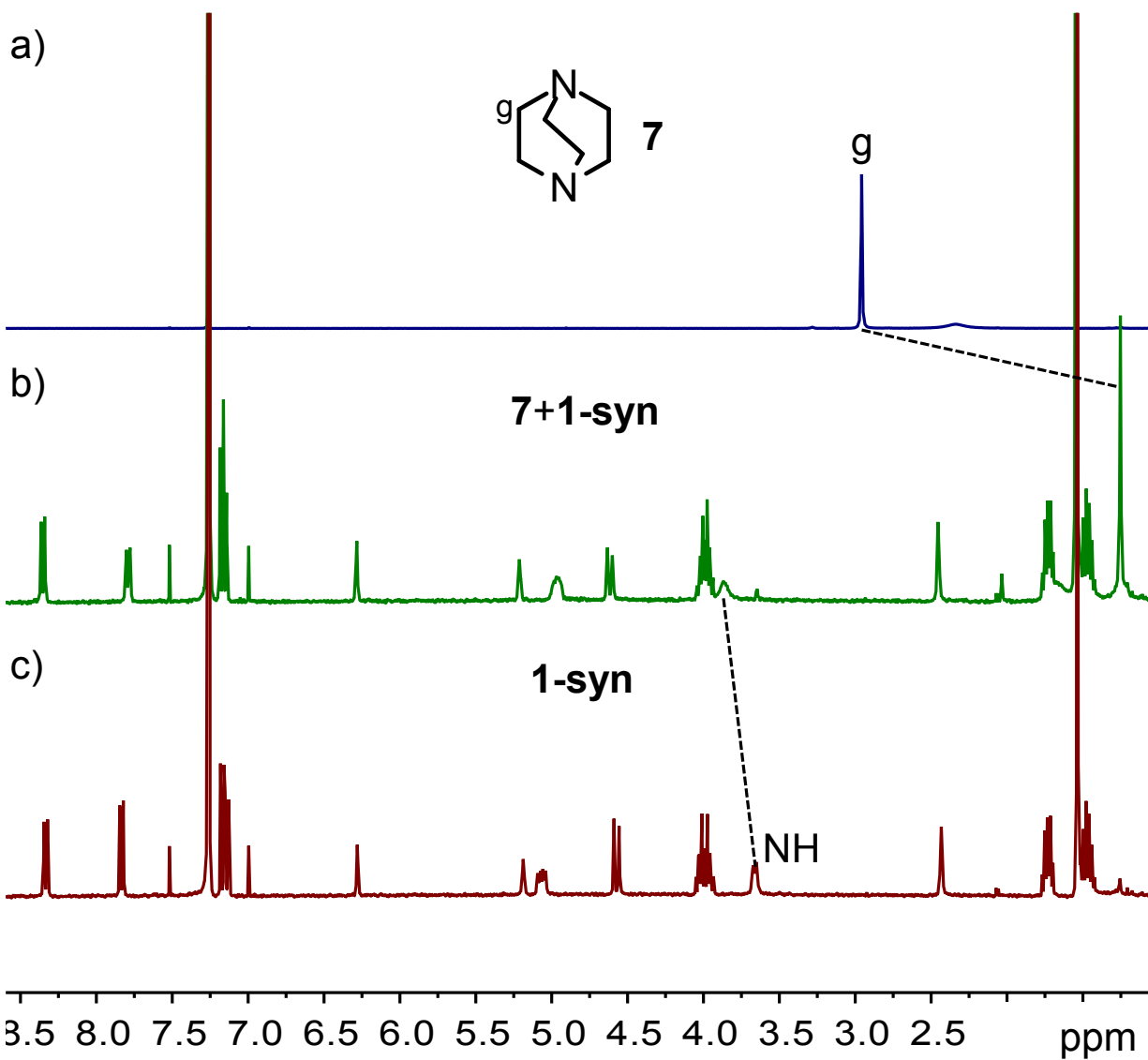


**Fig. S13**  $^1\text{H}$  NMR spectra (400 MHz,  $\text{CDCl}_3$ , 25  $^\circ\text{C}$ ) of (a) guest **7**, (c) **1-syn**, and (b) its equimolar mixture. The proton *g* of the guest experiences the large upfield shift, the proton NH of the host experiences the downfield shift, suggesting that the complexation between **1-syn** and guest **7**.

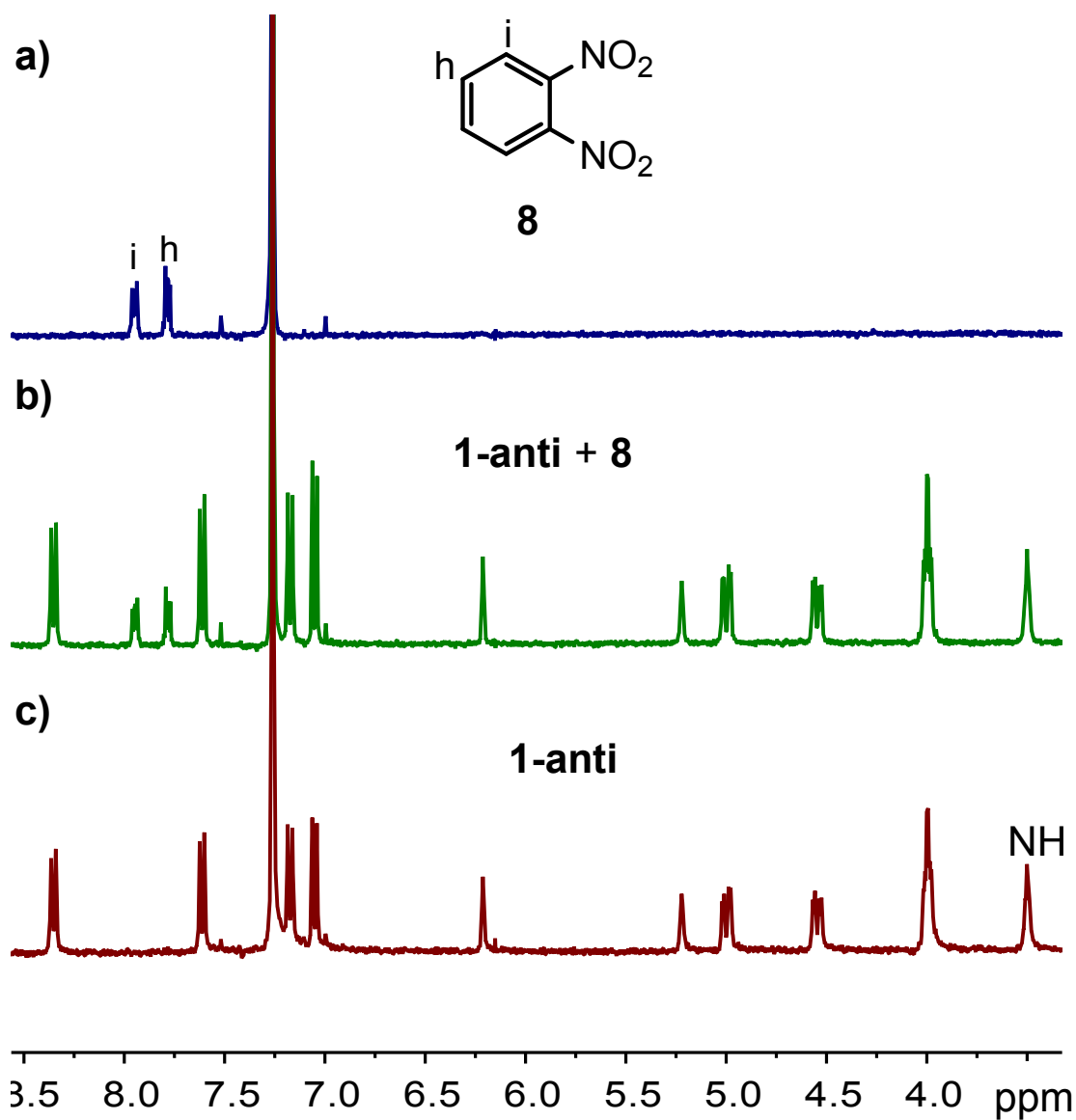


**Fig. S14** <sup>1</sup>H NMR spectra (400 MHz, CDCl<sub>3</sub>, 25 °C) of (a) guest **8**, (c) **1-anti**, and (b) its equimolar mixture. The protons *h* and *i* of the guest undergo no shift at all, suggesting no complexation between **1-anti** and guest **8**.

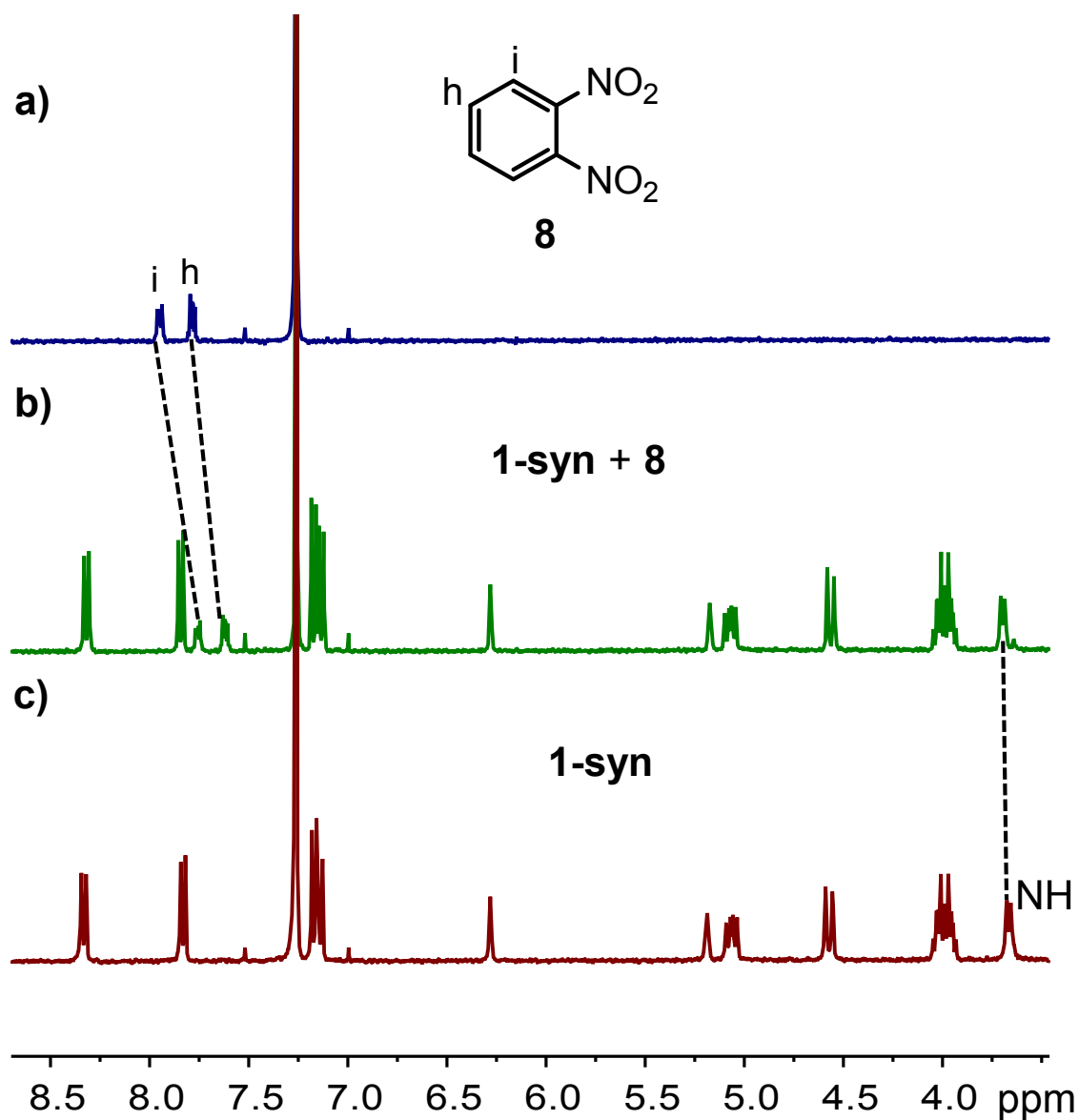


**Fig. S15** <sup>1</sup>H NMR spectra (400 MHz, CDCl<sub>3</sub>, 25 °C) of (a) guest **8**, (c) **1-syn**, and (b) its equimolar mixture. The protons *h* and *i* of the guest experiences the large upfield shift, suggesting that the complexation between **1-syn** and guest **8**.

## 6. Job's Plot and Determination of Binding Constants.

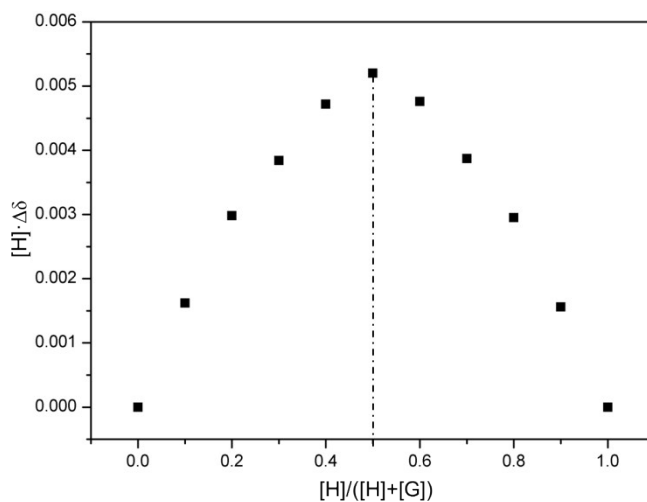


**Fig. S16** Job's plot obtained by plotting the chemical shift change ( $\Delta\delta$ ) of the Host's proton NH in  $^1\text{H}$  NMR spectra by varying the ratio of the host and the guest **4** against the mole fraction of Host **1-anti**. The total concentration of the host and the guest is fixed:  $[\text{Host}] + [\text{Guest}] = 1.0$  mM. This experiment supports the 1 : 1 binding stoichiometry between the guest **4** and **1-anti** in  $\text{CDCl}_3$ .

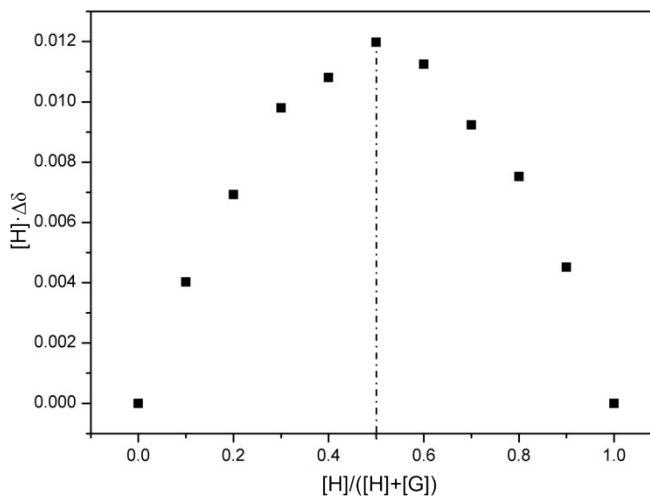


**Fig. S17** Job's plot obtained by plotting the chemical shift change ( $\Delta\delta$ ) of the Host's proton NH in  $^1\text{H}$  NMR spectra by varying the ratio of the host and the guest **4** against the mole fraction of Host **1-syn**. The total concentration of the host and the guest is fixed:  $[\text{Host}] + [\text{Guest}] = 1.0$  mM. This experiment supports the 1 : 1 binding stoichiometry between the guest **4** and **1-syn** in  $\text{CDCl}_3$ .

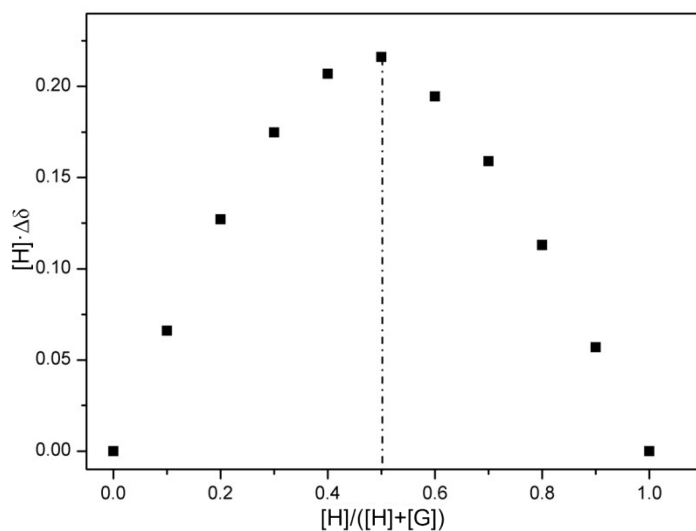


**Fig. S18** Job's plot obtained by plotting the chemical shift change ( $\Delta\delta$ ) of the Host's proton NH in  $^1\text{H}$  NMR spectra by varying the ratio of the host and the guest **7** against the mole fraction of Host **1-anti**. The total concentration of the host and the guest is fixed:  $[\text{Host}] + [\text{Guest}] = 1.0$  mM. This experiment supports the 1 : 1 binding stoichiometry between the guest **7** and **1-anti** in  $\text{CDCl}_3$ .

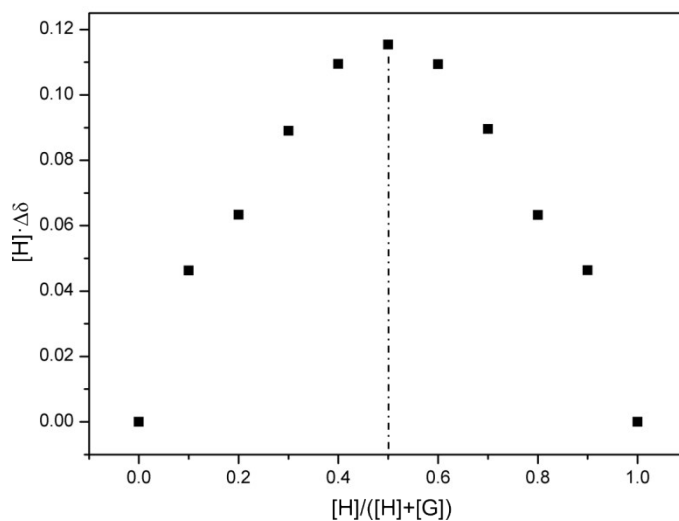


**Fig. S19** Job's plot obtained by plotting the chemical shift change ( $\Delta\delta$ ) of the Host's proton NH in  $^1\text{H}$  NMR spectra by varying the ratio of the host and the guest **7** against the mole fraction of Host **1-syn**. The total concentration of the host and the guest is fixed:  $[\text{Host}] + [\text{Guest}] = 1.0$  mM. This experiment supports the 1 : 1 binding stoichiometry between the guest **7** and **1-syn** in  $\text{CDCl}_3$ .



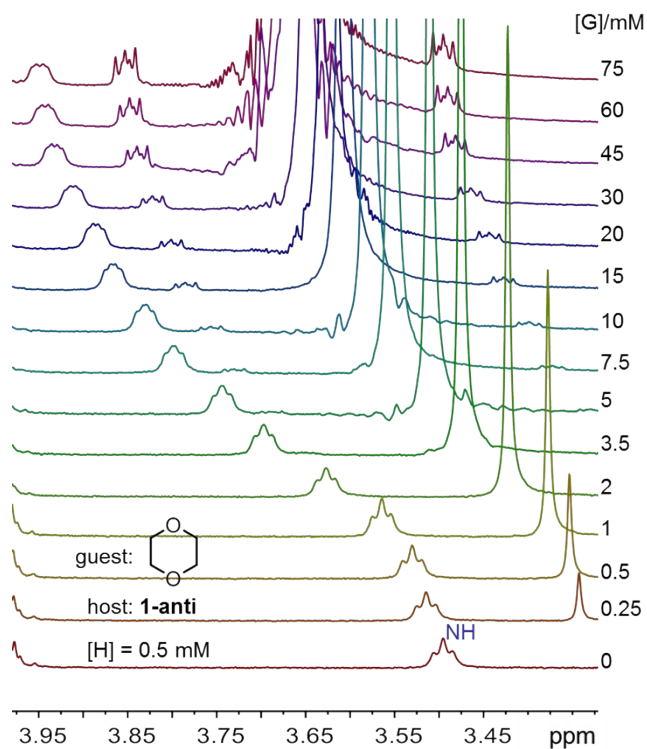


**Fig. S20** Partial <sup>1</sup>H NMR spectra (400 MHz, CDCl<sub>3</sub>, 25 °C) of **1-anti** (0.5 mM) titrated by the guest **4** (0~75.0 mM). Nonlinear curve-fitting method was then used to obtain the association constant through the following equation:

$$\delta = \delta_0 + \Delta\delta \cdot (0.5/[H]_0) \cdot ([G] + [H]_0 + 1/K - (([G] + [H]_0 + 1/K)^2 - 4[H]_0[G])^{0.5})$$

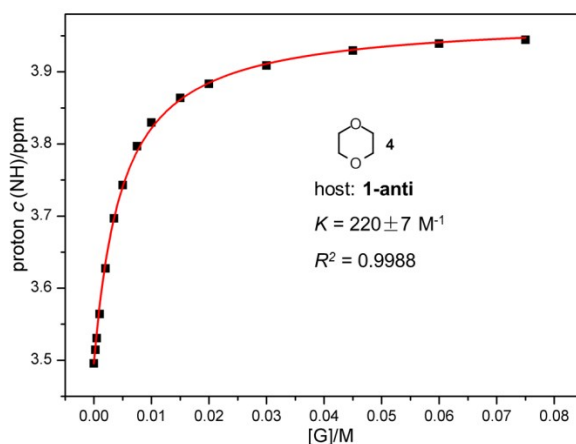


**Fig. S21** Non-linear curve-fitting for the complexation between **1-anti** and the guest **4** in CDCl<sub>3</sub> at 25 °C.

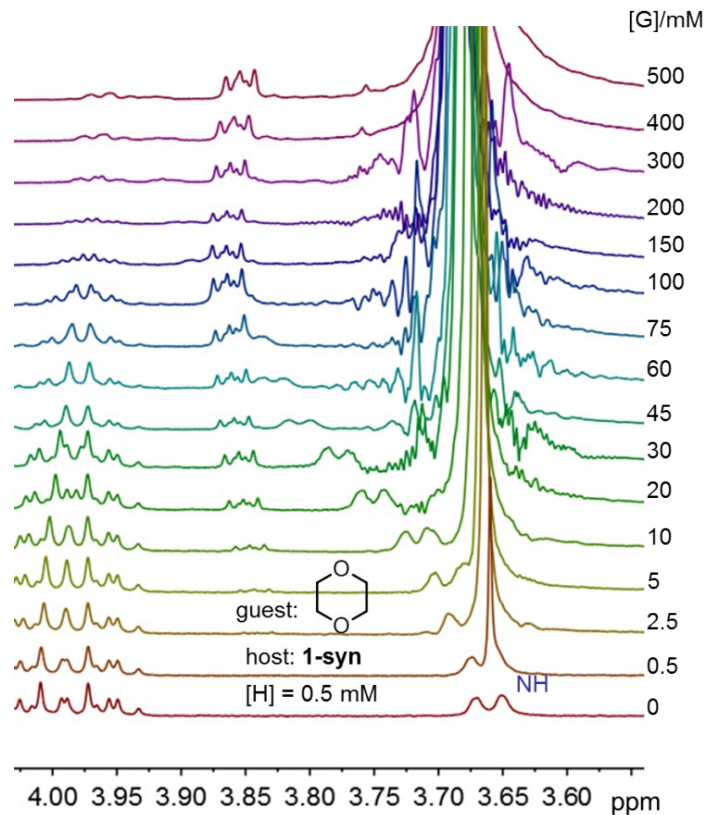


**Fig. S22** Partial  $^1\text{H}$  NMR spectra (400 MHz,  $\text{CDCl}_3$ , 25  $^\circ\text{C}$ ) of **1-syn** (0.5 mM) titrated by the guest **4** (0~500.0 mM).

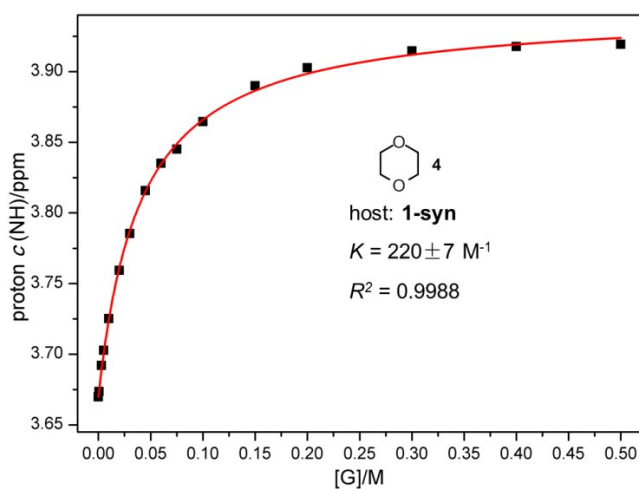


**Fig. S23** Non-linear curve-fitting for the complexation between **1-syn** and the guest **4** in  $\text{CDCl}_3$  at 25  $^\circ\text{C}$ .

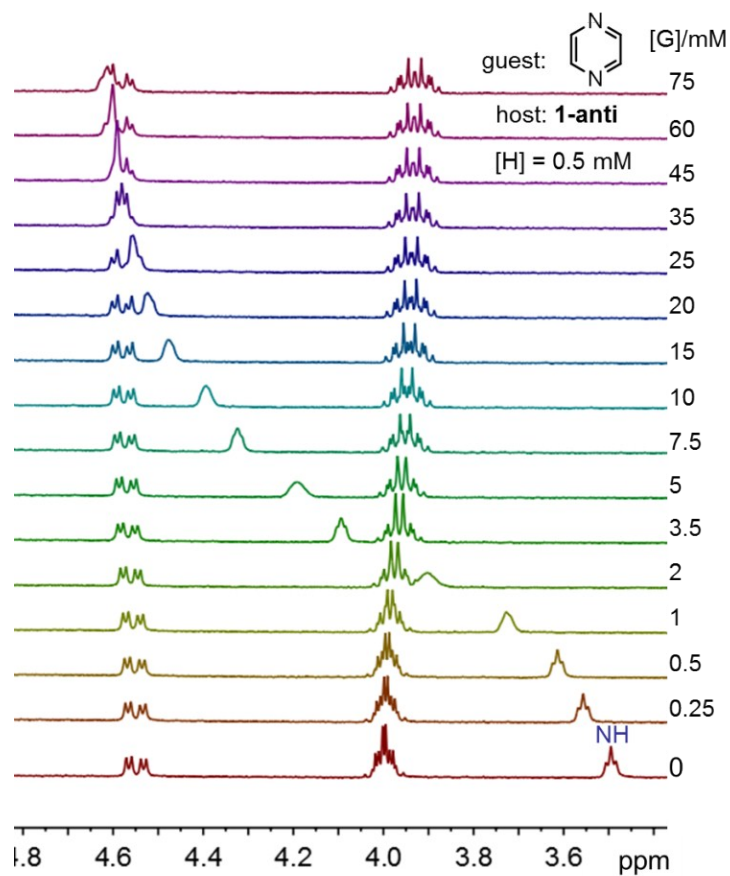


**Fig. S24** Partial <sup>1</sup>H NMR spectra (400 MHz, CDCl<sub>3</sub>, 25 °C) of **1-anti** (0.5 mM) titrated by the guest **5** (0~75.0 mM).

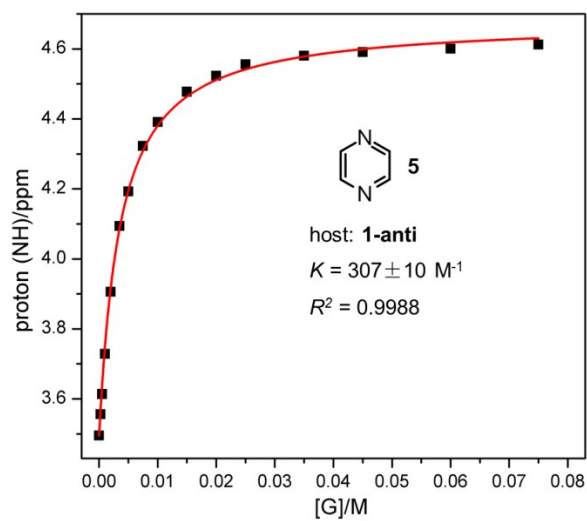


**Fig. S25** Non-linear curve-fitting for the complexation between **1-anti** and the guest **5** in CDCl<sub>3</sub> at 25 °C.

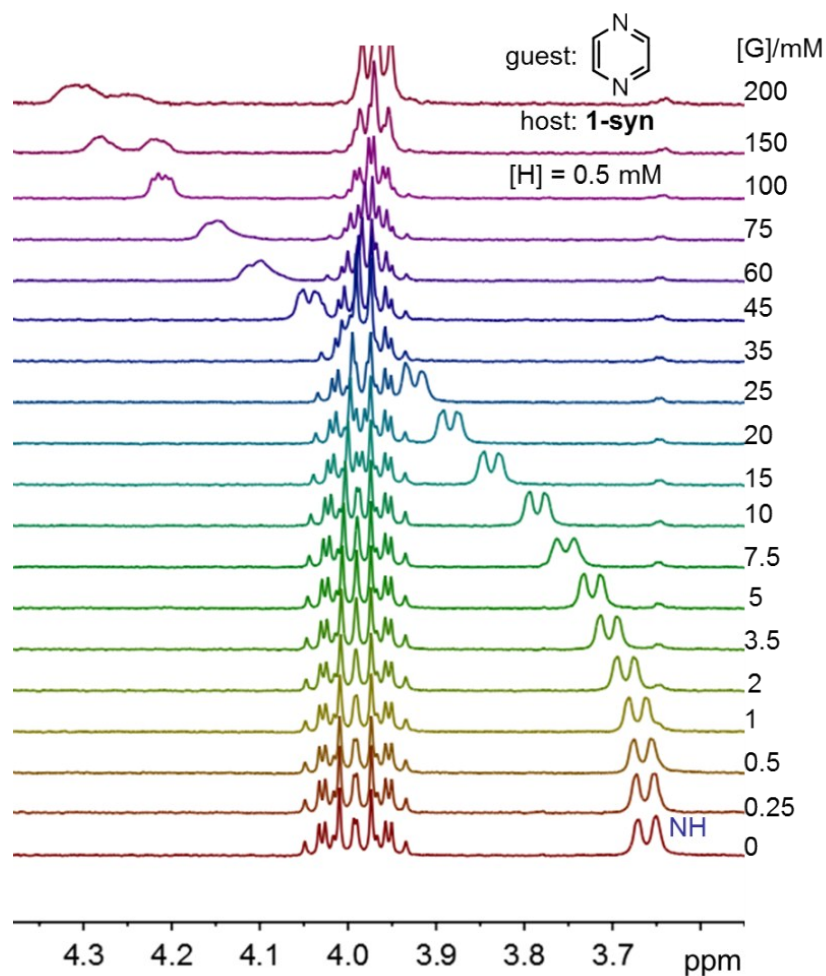


**Fig. S26** Partial  $^1\text{H}$  NMR spectra (400 MHz,  $\text{CDCl}_3$ , 25  $^\circ\text{C}$ ) of **1-syn** (0.5 mM) titrated by the guest **5** (0~200.0 mM).

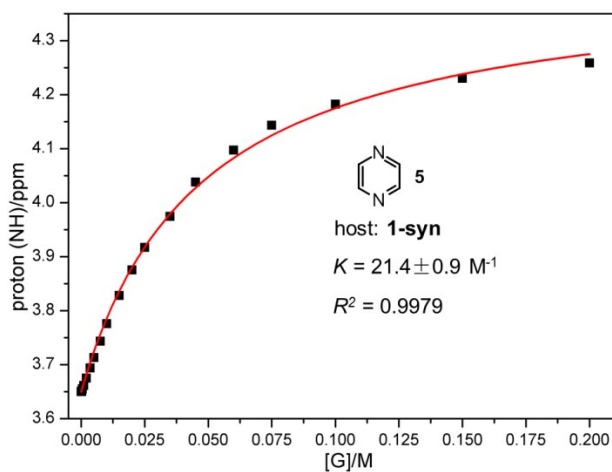


**Fig. S27** Non-linear curve-fitting for the complexation between **1-syn** and the guest **5** in  $\text{CDCl}_3$  at 25  $^\circ\text{C}$ .

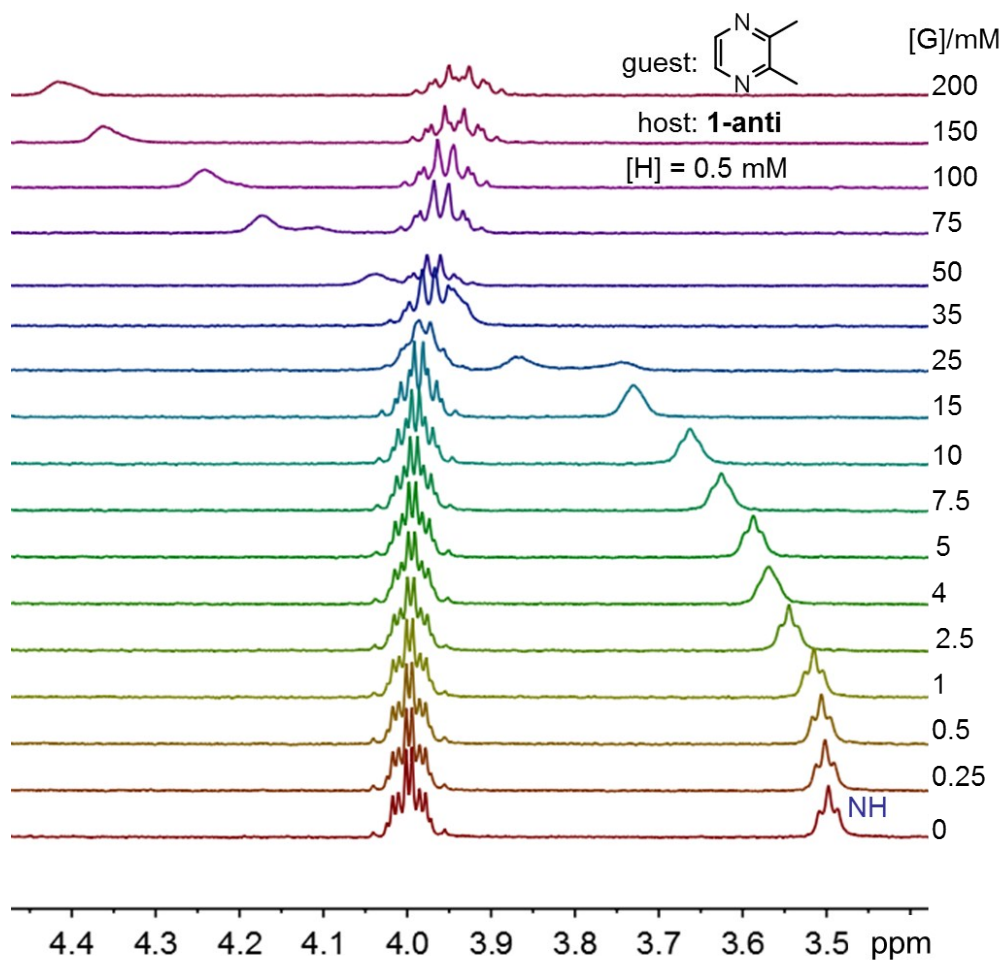


**Fig. S28** Partial  $^1\text{H}$  NMR spectra (400 MHz,  $\text{CDCl}_3$ , 25  $^\circ\text{C}$ ) of **1-anti** (0.5 mM) titrated by the guest **6** (0~200.0 mM).

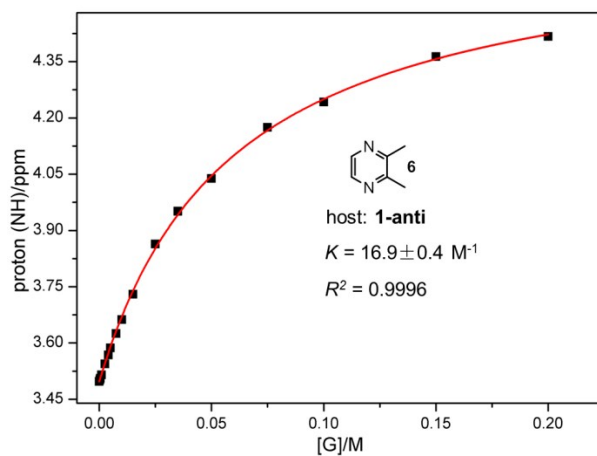


**Fig. S29** Non-linear curve-fitting for the complexation between **1-anti** and the guest **6** in  $\text{CDCl}_3$  at 25  $^\circ\text{C}$ .

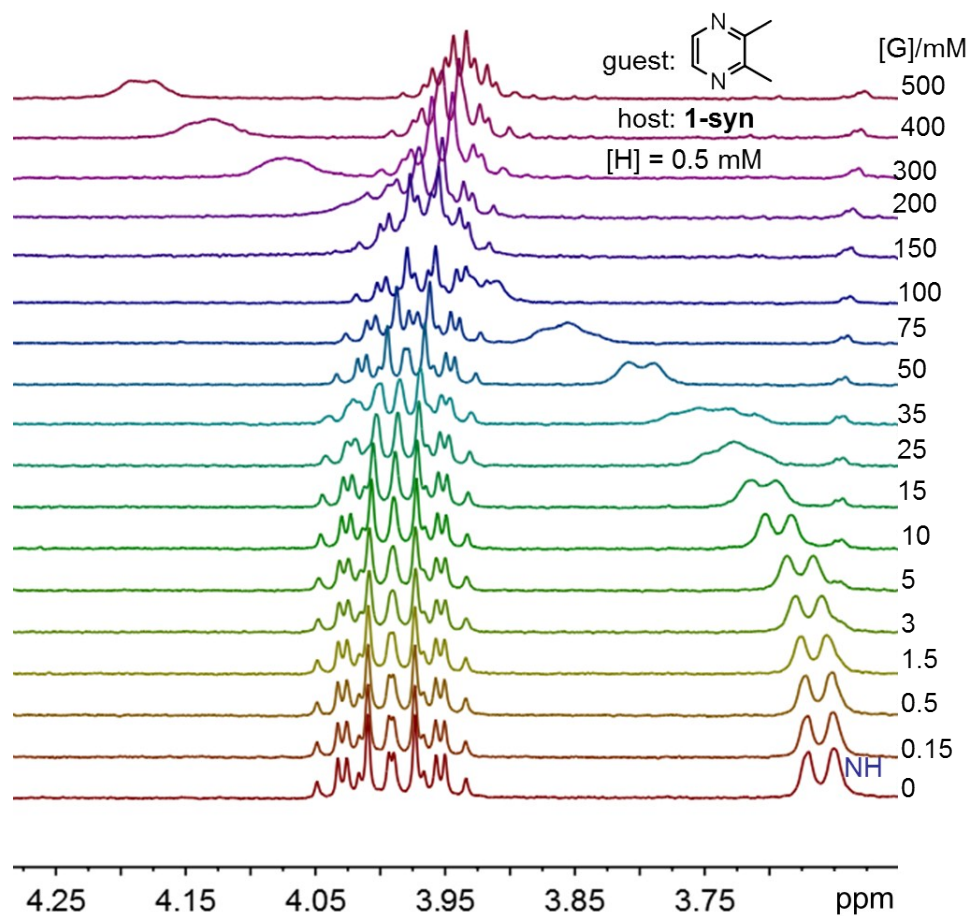


**Fig. S30** Partial <sup>1</sup>H NMR spectra (400 MHz, CDCl<sub>3</sub>, 25 °C) of **1-syn** (0.5 mM) titrated by the guest **6** (0~500.0 mM).

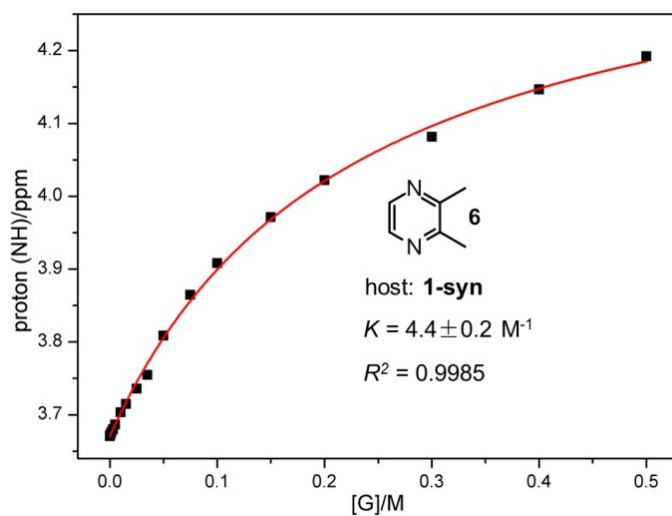


**Fig. S31** Non-linear curve-fitting for the complexation between **1-syn** and the guest **6** in CDCl<sub>3</sub> at 25 °C.

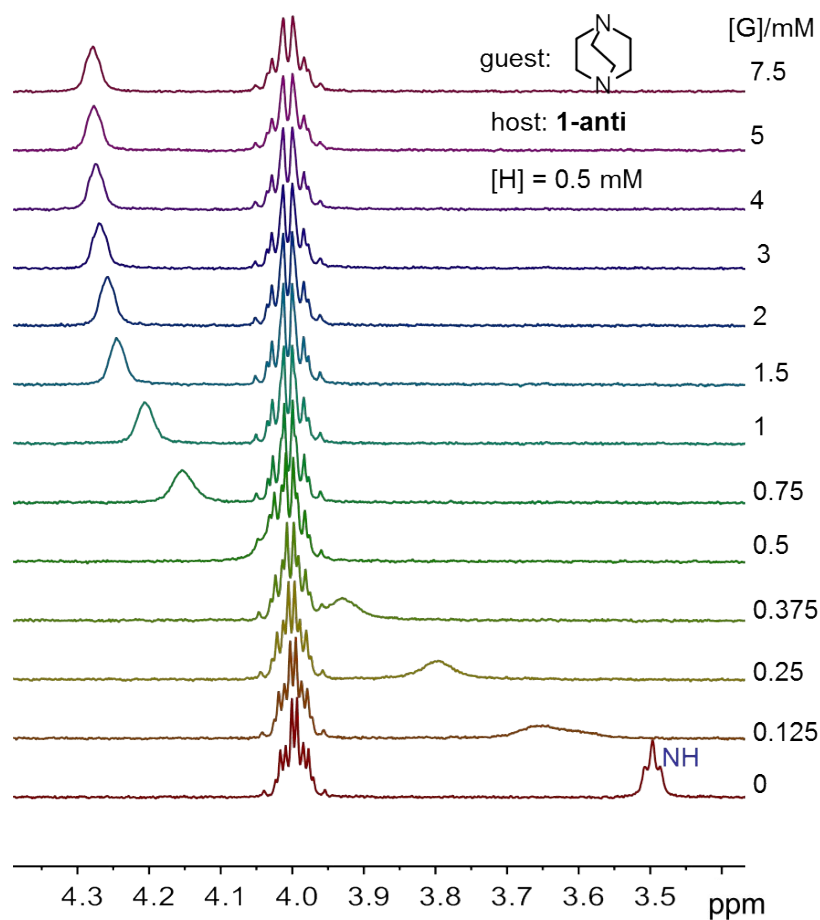


**Fig. S32** Partial <sup>1</sup>H NMR spectra (400 MHz, CDCl<sub>3</sub>, 25 °C) of **1-anti** (0.5 mM) titrated by the guest **7** (0~7.5 mM).

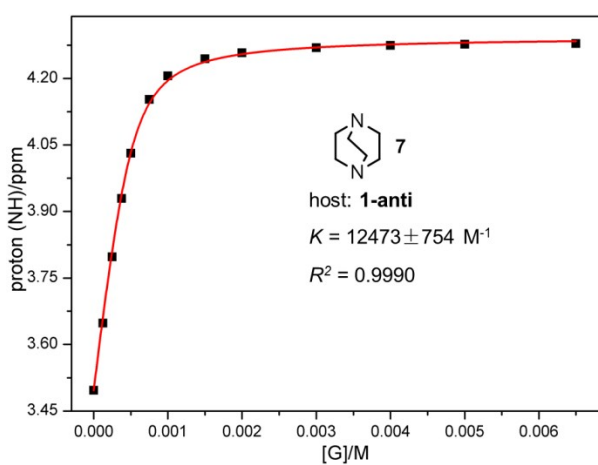


**Fig. S33** Non-linear curve-fitting for the complexation between **1-anti** and the guest **7** in CDCl<sub>3</sub> at 25 °C.

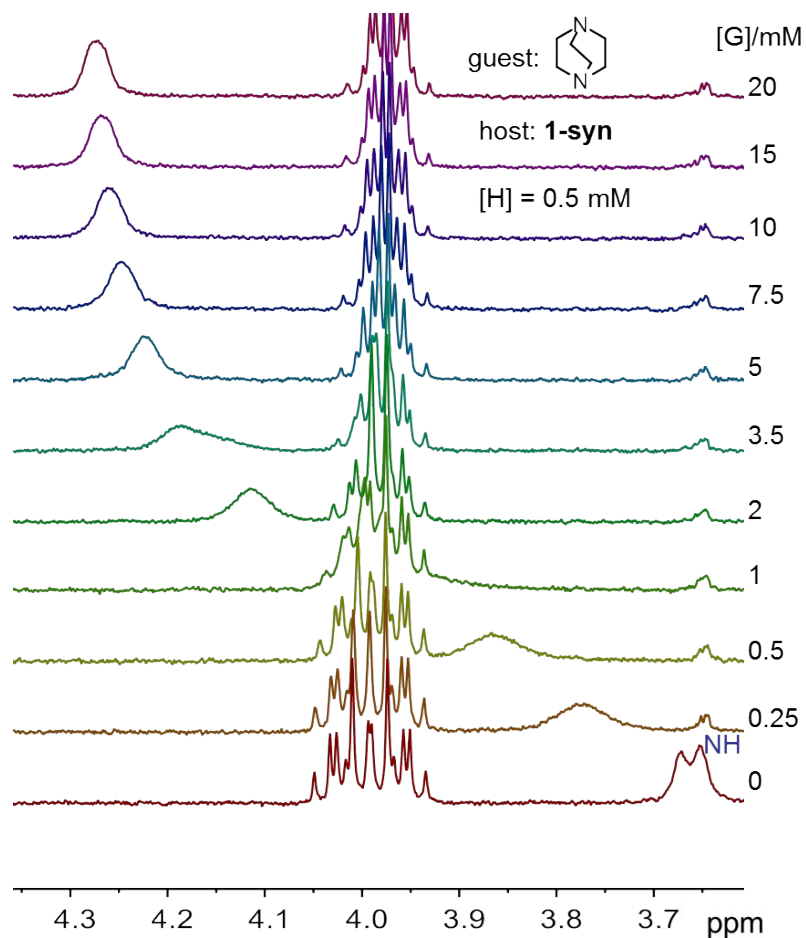


**Fig. S34** Partial  $^1\text{H}$  NMR spectra (400 MHz,  $\text{CDCl}_3$ , 25  $^\circ\text{C}$ ) of **1-syn** (0.5 mM) titrated by the guest **7** (0~20.0 mM).

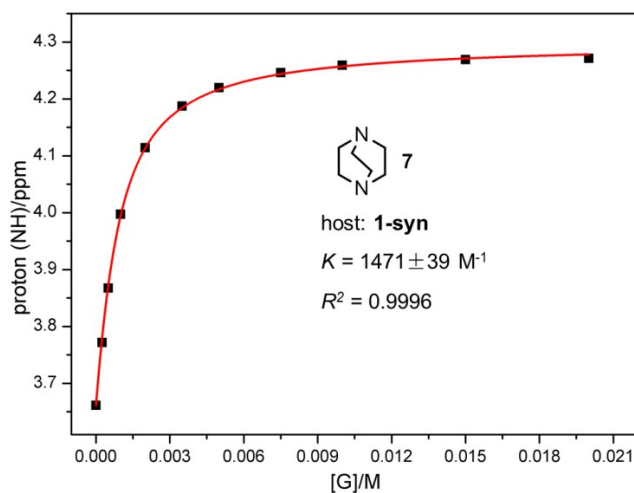


**Fig. S35** Non-linear curve-fitting for the complexation between **1-syn** and the guest **7** in  $\text{CDCl}_3$  at 25  $^\circ\text{C}$ .

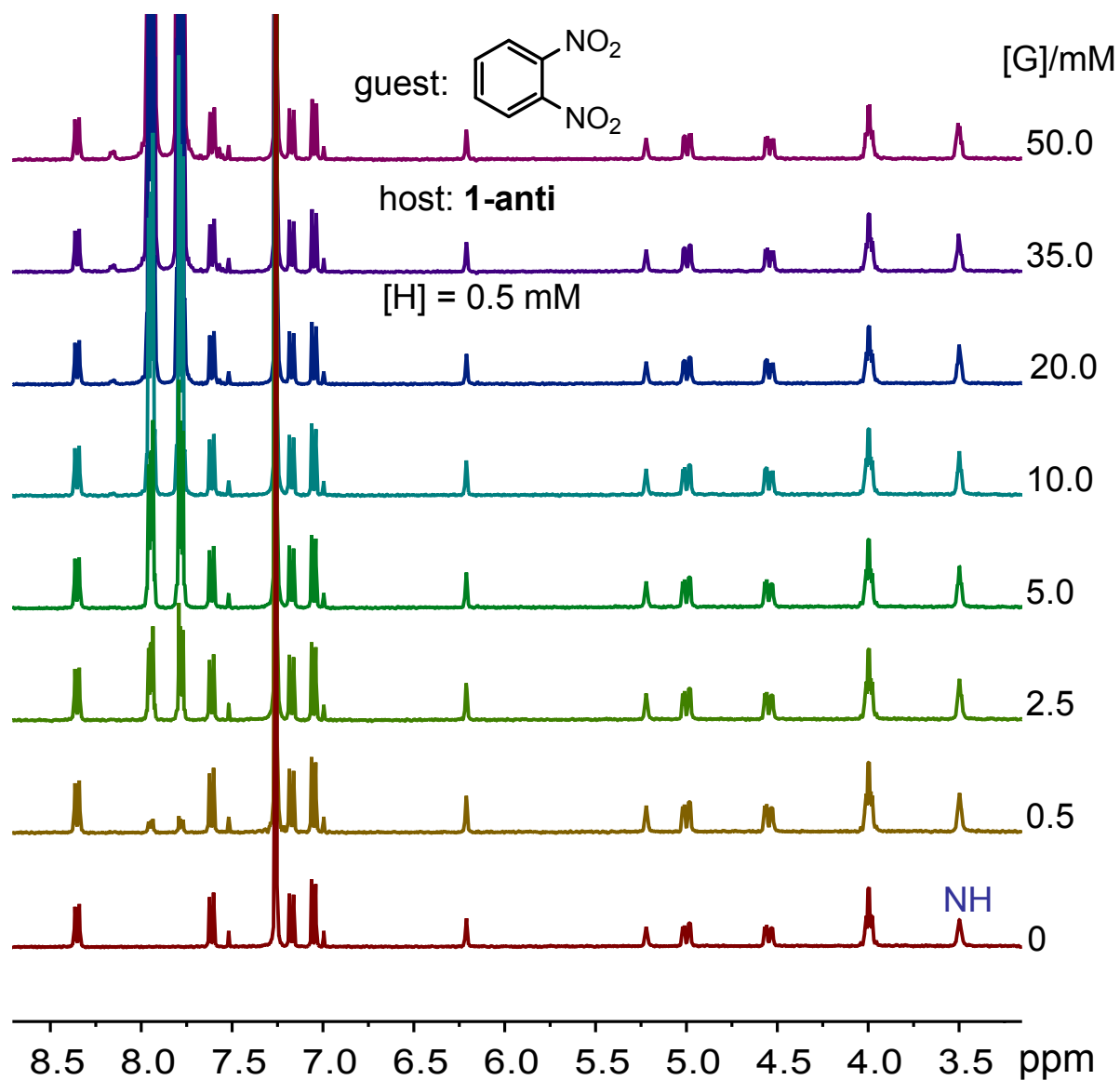


**Fig. S36** Partial  $^1\text{H}$  NMR spectra (400 MHz,  $\text{CDCl}_3$ , 25  $^\circ\text{C}$ ) of **1-syn** (0.5 mM) titrated by the guest **8** (0~20.0 mM). No obvious change on the  $^1\text{H}$  NMR spectra is observed, suggesting very weak binding between **8** and **1-anti** (likely  $< 1 \text{ M}^{-1}$ )

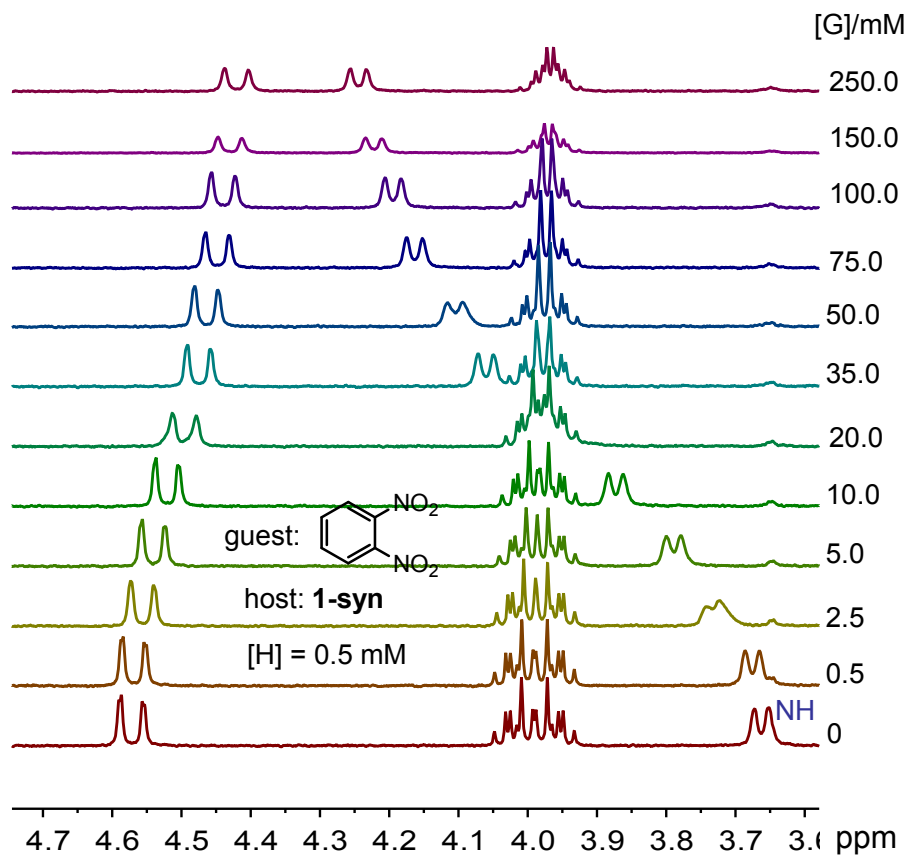


**Fig. S37** Partial  $^1\text{H}$  NMR spectra (400 MHz,  $\text{CDCl}_3$ , 25  $^\circ\text{C}$ ) of **1-syn** (0.5 mM) titrated by the guest **8** (0~250.0 mM).

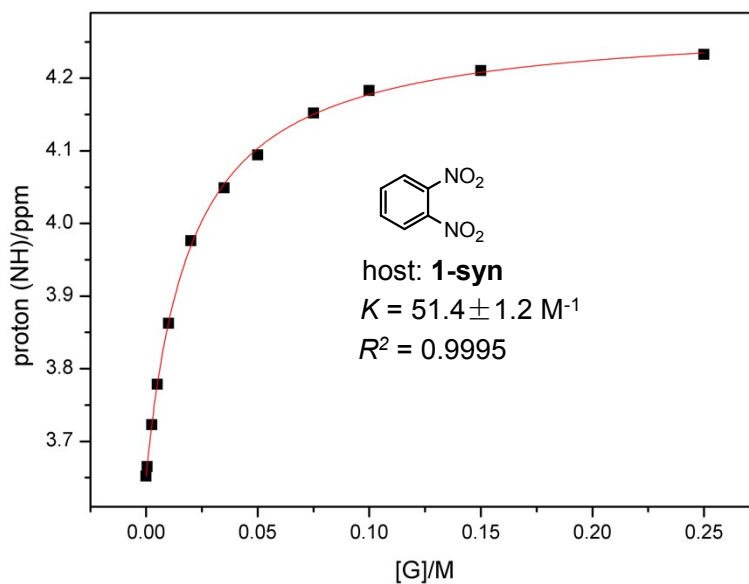


**Fig. S38** Non-linear curve-fitting for the complexation between **1-syn** and the guest **8** in  $\text{CDCl}_3$  at 25  $^\circ\text{C}$ .